THEORETICAL AND APPLIED MECHANICS
Article in Press (2026) DOI: https://doi.org/10.2298/TAM251127003D

STOCHASTIC STABILITY OF GYROSCOPIC VISCOELASTIC SYSTEMS AND APPLICATIONS IN AXIALLY MOVING BANDS

Jian Deng and Wei-Chau Xie

Abstract. This paper investigates the stochastic stability of gyroscopic viscoelastic systems subjected to parametric wide-band noise excitation. The analysis focuses on both moment stability, using moment Lyapunov exponents, and almost-sure stability, via the largest Lyapunov exponent. The wide-band noises considered include Gaussian white noise and Ornstein–Uhlenbeck noise. The Stratonovich stochastic differential equations governing the system with small damping and weak excitation are first converted to Itô stochastic differential equations through stochastic averaging techniques. An elegant mathematical framework is then introduced to approximate the moment Lyapunov exponents through stochastic transformations and an eigenvalue problem. The largest Lyapunov exponent is subsequently derived based on its relationship with the moment Lyapunov exponents. An application example involves deriving the stochastic equations of motion for an axially moving band system with fluctuating tension, analyzing its stochastic stability. The analytical approximations are validated via Monte Carlo simulations and compared with results from the literature. The study also discusses the influence of various parameters on the system's stability, with potential applications in engineering fields.

1. Introduction

For many mechanical and civil engineering structures, gyroscopic systems are usually an important component [1], and they can be modeled as:

$$\mathbf{M}\ddot{\mathbf{q}} + (\mathbf{D} + \mathbf{G})\dot{\mathbf{q}} + (\mathbf{K} + \mathbf{C})\mathbf{q} = 0, \tag{1.1}$$

where $\mathbf{q}$ is the vector of state coordinates, $\mathbf{M}$ is the inertial matrix, $\mathbf{D}$ is the viscous damping matrix, $\mathbf{G}$ is the gyroscopic matrix, $\mathbf{K}$ is the stiffness matrix with $\mathbf{K}^T = \mathbf{K}$, $\mathbf{C}$ is the circulatory matrix, $\mathbf{C}^T = -\mathbf{C}$, which is attributed to a non-conservative positional (circulatory) force. Eq. (1.1) is classified as gyroscopic because it contains the term $\mathbf{G}\dot{\mathbf{q}}$, where $\mathbf{G}$ is skew-symmetric, $\mathbf{G}^T = -\mathbf{G}$. The

2020 *Mathematics Subject Classification:* 37C75, 37N15.
Key words and phrases: stochastic stability, wide-band noise, viscoelasticity, axially moving band, moment Lyapunov exponents, largest Lyapunov exponent.

gyroscopic term often arises in rotating systems, where the equation of motion are expressed relative to the rotating body. These terms usually involve coupling between two or more coordinates.

The axially moving band under stochastically fluctuating tension is a typical gyroscopic system. The dynamic stability of axially moving systems has received considerable attention, partly because the characterization of vibrations and stability is essential for the analysis and optimal design of a broad class of mechanical systems that incorporate belt drives, chain drives, or moving bands. Due to irregular fluctuations, excessive wear and fatigue may occur in such systems, and the quality of products produced by these machines may become unpredictable.

One of the earliest studies on band saw vibrations was conducted by Mote [2], who obtained upper and lower bounds for the natural frequencies of transverse flexural vibration. Experimentally, Mote and Naguleswaran established a strong relationship between tension and axial velocity [3]. Around the same time, Naguleswaran and Williams [4] investigated the lateral vibration of moving bands caused by periodic tension fluctuations and derived conditions for parametric instability of the subharmonic type in flexural motion. Later, Ulsoy and Mote examined the vibration of wide-band saw blades using an axially moving plate model [5]. In a systematic study, Asokanthan analyzed the instability of torsional-flexural vibrations of band saws under deterministic periodic excitation and also investigated moment stability for both torsional and flexural vibrations under random tension fluctuations [6]. Yin [7] completed his master's thesis on Lyapunov exponents and the stochastic stability of linear gyroscopic systems—one of which was an axially moving band under stochastically fluctuating tension—using the method of stochastic averaging and Khasminskii's formulation [8]. More recently, Abdelrahman [9] obtained significant results for viscoelastic materials, including Lyapunov exponents and the stochastic stability of linear viscoelastic gyroscopic systems.

Loadings on structures can be of a deterministic [10–12] or stochastic nature [13–15]. The stability of stochastic systems can be analyzed using either sample-based or moment-based approaches [16]. Sample-based stochastic stability refers to almost-sure stability (i.e., stability with probability one), while moment-based stability concerns the behavior of the system's moments over time. Lyapunov exponents play a central role in characterizing almost-sure stability: the largest Lyapunov exponent not only determines whether a linear stochastic system is stable but also quantifies the exponential rate at which its solutions grow or decay over time. However, almost-sure (sample-path) stability does not necessarily imply moment stability. This distinction can be understood through the lens of large deviations theory [17]. For certain parameter values, the solution of a stochastic system may be almost surely stable, yet its second moment may still grow exponentially. Conversely, the second moment may remain stable, while higher-order moments, such as the fourth moment, grow exponentially. To fully understand the dynamic stability of a stochastic system, it is crucial to investigate both sample-path stability and moment stability for all real values of p. This requires evaluating both the largest Lyapunov exponent and the pth moment Lyapunov exponent, providing a comprehensive picture of the system's long-term behavior [14]. Moment

Lyapunov exponents provide information not only about moment stability but also about almost-sure stability.

Although moment Lyapunov exponents play a crucial role in the dynamic stability analysis of stochastic systems, their actual determination is very difficult—if not practically impossible to evaluate exactly. Therefore, several perturbation approximations [18] and asymptotic expansion series [19] have been developed for two-dimensional linear stochastic systems. Sri Namachchivaya and Van Roessel [20] investigated the moment Lyapunov exponents of two-degree-of-freedom (2DOF) coupled elastic oscillators under real noise excitations. Vedula completed his PhD thesis on the stability of parametrically excited linear and nonlinear gyroscopic systems [21], although viscoelasticity was not considered in his work. The moment Lyapunov exponents and the largest Lyapunov exponent for 2DOF coupled non-gyroscopic systems [22] and multiple-degree-of-freedom (MDOF) systems [23] have been derived using the stochastic averaging and the perturbation methods, respectively. More recently, a comprehensive book summarizing the author's group research on modeling complex dynamic systems, including stochastic stability, was published [15].

In many engineering structures, viscoelasticity is present in various materials [24], such as metals and alloys at elevated temperatures. Understanding the effect of viscoelasticity on structural stochastic stability is urgently needed due to the growing applications of viscoelastic materials. Although several studies have examined Lyapunov exponents in viscoelastic systems [9,25,26], relatively few have addressed moment Lyapunov exponents. Xie [27] derived a small-noise expansion for the moment Lyapunov exponent of a one-degree-of-freedom (1DOF) viscoelastic column under bounded noise excitation. Later, Huang and Xie [28] further investigated the moment Lyapunov exponents of such a viscoelastic system under wide-band noise excitation, using both first-and second-order stochastic averaging methods. It has been shown that special techniques are often required to address dynamic stability problems in viscoelastic structures [29].

To gain a comprehensive understanding of dynamic stability, it is essential to investigate both moment stability and almost-sure stability in gyroscopic viscoelastic systems subjected to wide-band noise excitations. This paper is motivated by the dynamic stability challenges encountered in axially moving viscoelastic bands exposed to stochastically fluctuating external loads. The main contributions and novelties of this study include: (1) the formulation of stochastic averaging for gyroscopic viscoelastic two-degree-of-freedom (2DOF) systems in Section 2. However, the detailed derivations are given in Appendix A and B; (2) a scheme for approximately determining the moment Lyapunov exponents and the largest Lyapunov exponent of gyroscopic systems using mathematical transformations only, presented in Section 3; (3) the calculation of analytical stability boundaries in Section 4; (4) an application to the stochastic stability analysis of axially moving viscoelastic bands in Section 5; (5) the formulation of a Monte Carlo simulation approach in Section 6; and (6) results and discussion provided in Section 7.

2. Formulation

Consider the following gyroscopic system of two-degree-of-freedom

$$\ddot{\mathbf{q}}+2\varepsilon\beta_a\dot{\mathbf{q}}+\varsigma\begin{bmatrix}0&-1\\1&0\end{bmatrix}\dot{\mathbf{q}}+\begin{bmatrix}k_1-\varepsilon\mathcal{H}&-\varepsilon\beta_b\varsigma\\\varepsilon\beta_b\varsigma&k_2-\varepsilon\delta\mathcal{H}\end{bmatrix}\mathbf{q}-\varepsilon^{1/2}\begin{bmatrix}1&0\\0&\zeta\end{bmatrix}\xi(t)\mathbf{q}=\mathbf{0}, \tag{2.1}$$

where $\mathbf{q}=\{q_1,q_2\}^T$ are state coordinates, β_a and β_b are damping coefficients, other parameters or coefficients are constants. There is a relationship $\beta_a=\beta_n+\beta_b$, where β_n and β_b denote the internal and external damping coefficients, respectively. $\varepsilon\ll 1$ is a small parameter introduced to make the analysis more convenient. $\mathcal{H}$ is a linear viscoelastic operator defined by

$$\mathcal{H}[\psi(t)]=\int_0^t H(t-\tau)\psi(\tau)\mathrm{d}\tau,\quad 0\leqslant\int_0^\infty H(\theta)\mathrm{d}\theta<1, \tag{2.2}$$

where $H(\theta)$ is the relaxation kernel. It is noted that Larionov [29] justified an averaging method in a rigorous manner for general integro-differential equations.

Random excitations $\xi(t)$ can be described as two types of wide-band stochastic processes [14]. The first is Gaussian white noise, formally defined as the time derivative of a Wiener process: $\xi(t)=\sigma\dot{W}(t)$ where σ is the intensity of the white noise. This process has a constant cosine power spectral density $S(\omega)=\sigma^2$ and a zero sine power spectral density $\Psi(\omega)=0$ across all frequencies. The second type, known as real noise, is often represented by an Ornstein–Uhlenbeck process, given by

$$\mathrm{d}\xi(t)=-\alpha\xi(t)\mathrm{d}t+\sigma\,\mathrm{d}W(t),$$

where $W(t)$ is a standard Wiener process. The corresponding power spectral densities are

$$S(\omega)=\frac{\sigma^2}{\alpha^2+\omega^2},\quad \Psi(\omega)=\frac{\omega\sigma^2}{\alpha(\alpha^2+\omega^2)}. \tag{2.3}$$

where σ and α are the parameters for intensity and band-width of the real noise, respectively. When α is large, the power of the real noise is spread across a wide frequency band. Therefore, the Ornstein–Uhlenbeck process can serve as a mathematical model for wide-band noise.

The equations of motion of many physical systems under the excitations of wide-band random processes can be approximated by Stratonovich stochastic differential equations. Eq. (2.1) is known as the Stratonovich stochastic differential equation if $\xi(t)$ is described as a wide-band stochastic process. A key advantage of this form is that it can be treated similarly to non-stochastic differential equations. However, physical stochastic processes are often approximated by Markov processes, in which case it is more convenient to use Itô stochastic differential equations [13, 30]. This approximation can be carried out using the method of stochastic averaging.

The process of applying the stochastic averaging method involves transforming the equations of motion in Eq. (2.1) from generalized coordinates to polar coordinates, as detailed in Appendix A. The transformation expresses the generalized coordinates ($q_1(t)$ and $q_2(t)$) in terms of amplitudes ($a_1(t)$ and $a_2(t)$), and phase angles ($\phi_1(t)$ and $\phi_2(t)$), using sinusoidal functions with frequencies (ω_1 and ω_2).

The specific transformation functions are given in Eq. (A.7), repeated here:

$$\begin{cases} q_1(t) = \varpi_{11} a_1(t) \sin[\omega_1 t + \phi_1(t)] + \varpi_{22}\, a_2(t) \sin[\omega_2 t + \phi_2(t)], \\ q_2(t) = \varpi_{11} a_1(t)\, \upsilon_1 \cos[\omega_1 t + \phi_1(t)] + \varpi_{22} a_2(t) \upsilon_2 \cos[\omega_2 t + \phi_2(t)], \end{cases} \tag{2.4}$$

where ϖ_{11} and ϖ_{22} are scaling parameters, ω_1 and ω_2 are the system's characteristic frequencies, υ_1 and υ_2 are constants defined in Eq. (A.5).

The equations of motion in Eq. (2.1) are transformed into differential equations for the amplitudes (a_i) and phase angles (ϕ_i) in Eq. (A.16), repeated here:

$$\dot{a}_i = \varepsilon^{1/2} F_{a,i}^{(0)} + \varepsilon F_{a,i}^{(1)}, \quad \dot{\phi}_i = \varepsilon^{1/2} F_{\phi,i}^{(0)} + \varepsilon F_{\phi,i}^{(1)}, \qquad i = 1, 2, \tag{2.5}$$

where $F_{a,i}^{(0)}$ and $F_{\phi,i}^{(0)}$ are functions containing the stochastic loads, $F_{a,i}^{(1)}$ and $F_{\phi,i}^{(1)}$ are functions without the stochastic loads. These four functions are derived in Eq. (A.17). In spite of the transformation from a second-order equation in Eq. (2.1) to a first-order equation in Eq. (2.5), all are still Stratonovich differential equations.

If the correlation function of the noise $\xi(t)$ decays sufficiently quickly to zero as the time t increases, then the Stratonovich stochastic differential equations $a_i(t)$ and $\phi_i(t)$ in Eq. (2.5) converge weakly on a time interval of order $1/\varepsilon$ to an Itô stochastic differential equation for the averaged amplitudes $\bar{a}_i$ and phase angles $\bar{\phi}_i$, whose solutions provide a uniformly valid first-order approximation to the exact values [13, 14, 30, 31]. As $\varepsilon \to 0$, the method of stochastic averaging could be applied to Eq. (2.5) to yield diffusive processes for the averaged amplitudes $\bar{a}_i(t)$ and phase angles $\bar{\phi}_i(t)$, $i = 1, 2$, in Eq. (B.1), repeated here:

$$\mathrm{d}a_i = \varepsilon m_i^a \mathrm{d}t + \varepsilon^{1/2} \sum_{j=1}^{2} \sigma_{ij}^a \mathrm{d}W_j^a, \tag{2.6a}$$

$$\mathrm{d}\phi_i = \varepsilon m_i^\phi \mathrm{d}t + \varepsilon^{1/2} \sum_{j=1}^{2} \sigma_{ij}^\phi \mathrm{d}W_j^\phi, \tag{2.6b}$$

where the overbar is removed for clarity of notations. $\mathbf{W}^a = \{W_1^a, W_2^a\}^T$ and $\mathbf{W}^\phi = \{W_1^\phi, W_2^\phi\}^T$ are two-dimensional vectors of independent standard Wiener processes. Stochastic averaging, the drift coefficients εm_i^a, εm_i^ϕ, and the elements of 2×2 diffusion matrices $\varepsilon \mathbf{b}^a = \varepsilon \boldsymbol{\sigma}^a (\boldsymbol{\sigma}^a)^T$, $\varepsilon \mathbf{b}^\phi = \varepsilon \boldsymbol{\sigma}^\phi (\boldsymbol{\sigma}^\phi)^T$, where $\boldsymbol{\sigma}^a = [\sigma_{ij}^a]$, $\boldsymbol{\sigma}^\phi = [\sigma_{ij}^\phi]$, $\mathbf{b}^a = [b_{ij}^a]$, $\mathbf{b}^\phi = [b_{ij}^\phi]$, are presented in Appendix B.

3. Moment stability and almost-sure stability

The sample, or almost-sure, stability of the stochastic system in Eq. (2.1) is governed by the largest Lyapunov exponents defined as

$$\lambda_{\mathbf{q}} = \lim_{t \to \infty} \frac{1}{t} \log \|\mathbf{q}\|,$$

where $\|\mathbf{q}\| = (\mathbf{q}^T \mathbf{q})^{1/2}$ is the Euclidean norm of the state coordinates. If the largest Lyapunov exponent is negative, the trivial solution of the system is stable with probability 1; otherwise, it is unstable almost surely.

On the other hand, the stability of the pth moment $\mathsf{E}[\|\mathbf{q}\|^p]$ of the solution of the system in Eq. (2.1) is governed by the pth moment Lyapunov exponent defined by

$$\Lambda_{\mathbf{q}}(p) = \lim_{t\to\infty} \frac{1}{t} \log \mathsf{E}[\|\mathbf{q}\|^p],$$

where $\mathsf{E}[\,\cdot\,]$ denotes the expected value. If $\Lambda_{\mathbf{q}}(\,p)$ is negative, then the pth moment is stable; otherwise, it is unstable.

It is important to note that the original equation of motion in Eq. (2.1) has been deliberately approximated by Eq. (2.6a) and (2.6b) through the method of stochastic averaging. Both the averaged amplitude equation a_i in Eq. (2.6a) and the phase angle equation ϕ_i in Eq. (2.6b) do not involve the phase angles, so the amplitude equations are advantageously decoupled from the phase angle equations. Hence, the averaged amplitude vector $(a_1,\, a_2)$ is a two-dimensional diffusion process, on which the moment Lyapunov exponents will be formulated through stochastic transformations and an eigenvalue problem in the next section.

3.1. Stochastic transformations. For a two-dimensional amplitude system such as Eq. (2.6a), an approach has been developed to obtain moment Lyapunov exponents [32]. For completeness, that approach is outlined here.

First, one may transform the Itô stochastic differential equations for the amplitudes using Khasminskii's transformation as follows [8, 36]:

$$r = \sqrt{a_1^2 + a_2^2}, \quad \varphi = \tan^{-1}\frac{a_2}{a_1}, \quad a_1 = r\cos\varphi, \quad a_2 = r\sin\varphi, \quad P = r^p, \tag{3.1}$$

and then the moment Lyapunov exponent is given by

$$\Lambda = \lim_{t\to\infty} \frac{1}{t} \log \mathsf{E}[P].$$

The Itô stochastic differential equations for P and φ can be obtained using the Itô Lemma,

$$\mathrm{d}P = m_P(P,\varphi)\mathrm{d}t + \sigma_{P1}\mathrm{d}W_1 + \sigma_{P2}\,\mathrm{d}W_2 = m_P(P,\varphi)\mathrm{d}t + \Sigma_P(P,\varphi)\mathrm{d}W, \tag{3.2}$$

$$\mathrm{d}\varphi = m_\varphi(\varphi)\mathrm{d}t + \sigma_{\varphi 1}\mathrm{d}W_1 + \sigma_{\varphi 2}\mathrm{d}W_2 = m_\varphi(\varphi)\mathrm{d}t + \Sigma_\varphi(\varphi)\mathrm{d}W, \tag{3.3}$$

where

$$\begin{aligned} m_P(P,\varphi) &= \varepsilon\Big\{ m_1^a \frac{\partial P}{\partial a_1} + m_2^a \frac{\partial P}{\partial a_2} + \frac{1}{2}\Big[b_{11}^a \frac{\partial^2 P}{\partial a_1^2} + (b_{12}^a + b_{21}^a)\frac{\partial^2 P}{\partial a_1 \partial a_2} + b_{22}^a \frac{\partial^2 P}{\partial a_2^2}\Big]\Big\} \\ &= \varepsilon p P\Big\{ \frac{m_1^a}{\sqrt{a_1^2+a_2^2}}\cos\varphi + \frac{m_2^a}{\sqrt{a_1^2+a_2^2}}\sin\varphi + \frac{1}{2}\Big[\frac{b_{11}^a}{a_1^2+a_2^2}[(p-2)\cos^2\varphi + 1] \\ &\qquad + \frac{(b_{12}^a + b_{21}^a)}{2(a_1^2+a_2^2)}(p-2)\sin 2\varphi + \frac{b_{22}^a}{a_1^2+a_2^2}[(p-2)\sin^2\varphi + 1]\Big]\Big\}, \end{aligned} \tag{3.4}$$

$$\Sigma_P^2 = \sigma_{P1}^2 + \sigma_{P2}^2 = \varepsilon \begin{Bmatrix} \sigma_{11}^a \dfrac{\partial P}{\partial a_1} + \sigma_{21}^a \dfrac{\partial P}{\partial a_2} & \sigma_{12}^a \dfrac{\partial P}{\partial a_1} + \sigma_{22}^a \dfrac{\partial P}{\partial a_2} \end{Bmatrix} \begin{Bmatrix} \sigma_{11}^a \dfrac{\partial P}{\partial a_1} + \sigma_{21}^a \dfrac{\partial P}{\partial a_2} \\ \sigma_{12}^a \dfrac{\partial P}{\partial a_1} + \sigma_{22}^a \dfrac{\partial P}{\partial a_2} \end{Bmatrix}$$

$$= \varepsilon\Big[((\sigma_{11}^a)^2 + (\sigma_{12}^a)^2)\Big(\frac{\partial P}{\partial a_1}\Big)^2 + 2(\sigma_{11}^a\sigma_{21}^a + \sigma_{12}^a\sigma_{22}^a)\frac{\partial P}{\partial a_1}\frac{\partial P}{\partial a_2} + ((\sigma_{21}^a)^2 + (\sigma_{22}^a)^2)\Big(\frac{\partial P}{\partial a_2}\Big)^2\Big]$$
$$= \varepsilon\Big[b_{11}^a\Big(\frac{\partial P}{\partial a_1}\Big)^2 + (b_{12}^a + b_{21}^a)\frac{\partial P}{\partial a_1}\frac{\partial P}{\partial a_2} + b_{22}^a\Big(\frac{\partial P}{\partial a_2}\Big)^2\Big],$$

$$m_\varphi(\varphi) = \varepsilon\Big\{m_1^a\frac{\partial\varphi}{\partial a_1} + m_2^a\frac{\partial\varphi}{\partial a_2} + \frac{1}{2}\Big[b_{11}^a\frac{\partial^2\varphi}{\partial a_1^2} + (b_{12}^a + b_{21}^a)\frac{\partial^2\varphi}{\partial a_1\partial a_2} + b_{22}^a\frac{\partial^2\varphi}{\partial a_2^2}\Big]\Big\} \tag{3.5}$$
$$= \varepsilon\Big\{-\frac{m_1^a}{\sqrt{a_1^2+a_2^2}}\sin\varphi + \frac{m_2^a}{\sqrt{a_1^2+a_2^2}}\cos\varphi + \frac{1}{2}\Big[\frac{b_{11}^a}{a_1^2+a_2^2}\sin 2\varphi - \frac{(b_{12}^a + b_{21}^a)}{a_1^2+a_2^2}(2\cos^2\varphi - 1) - \frac{b_{22}^a}{a_1^2+a_2^2}\sin 2\varphi\Big]\Big\},$$

$$\Sigma_\varphi^2 = \sigma_{\varphi 1}^2 + \sigma_{\varphi 2}^2 = \varepsilon\Big[b_{11}^a\Big(\frac{\partial\varphi}{\partial a_1}\Big)^2 + (b_{12}^a + b_{21}^a)\frac{\partial\varphi}{\partial a_1}\frac{\partial\varphi}{\partial a_2} + b_{22}^a\Big(\frac{\partial\varphi}{\partial a_2}\Big)^2\Big] \tag{3.6}$$
$$= \varepsilon\Big[\frac{b_{11}^a}{a_1^2+a_2^2}\sin^2\varphi - \frac{(b_{12}^a + b_{21}^a)}{a_1^2+a_2^2}\sin\varphi\cos\varphi + \frac{b_{22}^a}{a_1^2+a_2^2}\cos^2\varphi\Big].$$

It is noted that the coefficients of the terms on the right-hand side of the amplitude equations in Eq. (2.6a), such as m_i^a for $i = 1, 2$, are homogeneous of degree one in a_1 and a_2. This implies that the diffusion term $\mathbf{b}^a$ in Eq. (B.2) are homogeneous of degree two in a_1 and a_2.

Therefore, substituting $a_1 = r\cos\varphi$ and $a_2 = r\sin\varphi$ from Eq. (3.1) into Eq. (3.4), one finds that the drift term $m_P(P,\varphi)$ and the diffusion term $\Sigma_P(P,\varphi)$ are functions of P of degree one and of φ.

However, the drift term $m_\varphi(\varphi)$ in Eq. (3.5) and the diffusion term $\Sigma_\varphi(\varphi)$ in Eq. (3.6) are functions of φ only. This shows that $P(t)$ in Eq. (3.2) and $\varphi(t)$ in Eq. (3.3) are coupled, although $\varphi(t)$ is itself a diffusion process.

A linear stochastic transformation is then applied [36]

$$Q = T(\varphi)P, \quad P = T^{-1}(\varphi)Q, \qquad 0 \leqslant \varphi < \pi,$$

from which the following partial derivatives are obtained:

$$\frac{\partial Q}{\partial P} = T(\varphi), \quad \frac{\partial Q}{\partial\varphi} = T'_\varphi P, \quad \frac{\partial^2 Q}{\partial P^2} = 0, \quad \frac{\partial^2 Q}{\partial P\partial\varphi} = T'_\varphi, \quad \frac{\partial^2 Q}{\partial^2\varphi} = PT''_{\varphi\varphi},$$

where T'_φ and $T''_{\varphi\varphi}$ denote the first-order and second-order derivative of $T(\varphi)$ with respect to φ, respectively.

The Itô stochastic differential equation for the transformed pth norm process Q can also be derived using Itô's Lemma

$$\mathrm{d}Q = m_Q\,\mathrm{d}t + \Big(\sigma_{P1}\frac{\partial Q}{\partial P}\mathrm{d}W_1 + \sigma_{P2}\frac{\partial Q}{\partial P}\mathrm{d}W_2 + \sigma_{\varphi 1}\frac{\partial Q}{\partial\varphi}\mathrm{d}W_1 + \sigma_{\varphi 2}\frac{\partial Q}{\partial\varphi}\mathrm{d}W_2\Big), \tag{3.7}$$

where the drift coefficient is given by

$$m_Q = m_P\frac{\partial Q}{\partial P} + m_\varphi\frac{\partial Q}{\partial\varphi} + \frac{1}{2}\Big[b_{11}^Q\frac{\partial^2 Q}{\partial P^2} + (b_{12}^Q + b_{21}^Q)\frac{\partial^2 Q}{\partial P\partial\varphi} + b_{22}^Q\frac{\partial^2 Q}{\partial\varphi^2}\Big]$$
$$= \frac{1}{2}P(\sigma_{\varphi 1}^2 + \sigma_{\varphi 2}^2)T''_{\varphi\varphi} + (m_\varphi P + \sigma_{P1}\sigma_{\varphi 1} + \sigma_{P2}\sigma_{\varphi 2})T'_\varphi + m_P T,$$

and the diffusion terms satisfy the relationship

$$\mathbf{b}^Q = \left[\sigma^Q (\sigma^Q)^T\right], \quad \sigma^Q = \begin{bmatrix} \sigma_{P1} & \sigma_{P2} \\ \sigma_{\varphi 1} & \sigma_{\varphi 2} \end{bmatrix}. \tag{3.8}$$

Substituting σ_{P1}, σ_{P2}, $\sigma_{\varphi 1}$, and $\sigma_{\varphi 2}$ into Eq. (3.8) leads to

$$b_{11}^Q = \sigma_{P1}^2 + \sigma_{P2}^2 = \Sigma_P^2, \quad b_{22}^Q = \sigma_{\varphi 1}^2 + \sigma_{\varphi 2}^2 = \Sigma_\varphi^2, \tag{3.9}$$

$$\begin{aligned} b_{12}^Q = b_{21}^Q &= \sigma_{P1}\sigma_{\varphi 1} + \sigma_{P2}\sigma_{\varphi 2} \\ &= \varepsilon[(\sigma_{11}^a)^2 + (\sigma_{12}^a)^2]\frac{\partial P}{\partial a_1}\frac{\partial \varphi}{\partial a_1} + \varepsilon(\sigma_{11}^a\sigma_{21}^a + \sigma_{12}^a\sigma_{22}^a)\Big[\frac{\partial P}{\partial a_1}\frac{\partial \varphi}{\partial a_2} + \frac{\partial P}{\partial a_2}\frac{\partial \varphi}{\partial a_1}\Big] \\ &\quad + \varepsilon[(\sigma_{21}^a)^2 + (\sigma_{22}^a)^2]\frac{\partial P}{\partial a_2}\frac{\partial \varphi}{\partial a_2} \\ &= \varepsilon\Big\{b_{11}^a\frac{\partial P}{\partial a_1}\frac{\partial \varphi}{\partial a_1} + b_{12}^a\Big[\frac{\partial P}{\partial a_1}\frac{\partial \varphi}{\partial a_2} + \frac{\partial P}{\partial a_2}\frac{\partial \varphi}{\partial a_1}\Big] + b_{22}^a\frac{\partial P}{\partial a_2}\frac{\partial \varphi}{\partial a_2}\Big\} \\ &= \varepsilon p P\Big[-\frac{b_{11}^a}{a_1^2+a_2^2}\cos\varphi\sin\varphi + \frac{b_{12}^a}{a_1^2+a_2^2}(\cos^2\varphi - \sin^2\varphi) + \frac{b_{22}^a}{a_1^2+a_2^2}\cos\varphi\sin\varphi\Big]. \end{aligned} \tag{3.10}$$

For a bounded and non-singular transformation $T(\varphi)$, both processes P and Q are expected to exhibit the same stability behaviour. Therefore, the transformation $T(\varphi)$ is chosen such that the drift term in the Itô differential equation (3.7) becomes independent of the phase process φ, resulting in the simplified stochastic differential equation:

$$\mathrm{d}Q = \varepsilon\Lambda Q\mathrm{d}t + \varepsilon^{1/2}(\sigma_{Q1}\mathrm{d}W_1 + \sigma_{Q2}\mathrm{d}W_2). \tag{3.11}$$

By comparing the drift terms in Eqs. (3.7) and (3.11), one finds that the transformation $T(\varphi)$ must satisfy the following equation, i.e., the eigenvalue problem,

$$\frac{1}{2}P(\sigma_{\varphi 1}^2 + \sigma_{\varphi 2}^2)T''_{\varphi\varphi} + (m_\varphi P + \sigma_{P1}\sigma_{\varphi 1} + \sigma_{P2}\sigma_{\varphi 2})T'_\varphi + m_P T = \varepsilon\Lambda T, \quad 0 \leqslant \varphi < \pi, \tag{3.12}$$

where $T(\varphi)$ is a periodic function in φ with period π. Eq. (3.12) thus defines an eigenvalue problem for a second-order differential operator, with Λ being the eigenvalue and $T(\varphi)$ the associated eigenfunction.

Taking the expected value of both sides of Eq. (3.11), and noting that $\mathsf{E}[\sigma_{Q1}\mathrm{d}W_1 + \sigma_{Q2}\mathrm{d}W_2] = 0$ [14], one obtains $\mathsf{E}[Q] = \varepsilon\Lambda\mathsf{E}[Q]\mathrm{d}t$, from which it follows that the eigenvalue Λ corresponds to the Lyapunov exponent of the pth moment of system (2.1), i.e., $\Lambda = \Lambda_{\mathbf{q}(t)}(p)$.

Substituting Eqs. (3.9) and (3.10) into Eq. (3.12) yields

$$\mathcal{L}(p)[T] = \frac{1}{P}\Big\{\frac{1}{2}\Sigma_\varphi^2 P T''_{\varphi\varphi} + [m_\varphi P + b_{12}^Q]T'_\varphi + m_P T\Big\} = \varepsilon\Lambda T, \quad 0 \leqslant \varphi < \pi, \tag{3.13}$$

where Σ_φ^2, m_φ, b_{12}^Q, and m_P are given in (3.6), (3.5), (3.10), and (3.4), respectively. Substituting these four equations into Eq. (3.13) yields

$$\mathcal{L}(p)[T] = \lambda_2 T''_{\varphi\varphi} + \lambda_1 T'_\varphi + \lambda_0 T = \Lambda T, \quad 0 \leqslant \varphi < \pi, \tag{3.14}$$

where

$$\lambda_2 = \frac{1}{2}\Big[\frac{b_{11}^a}{a_1^2+a_2^2}\sin^2\varphi - \frac{(b_{12}^a+b_{21}^a)}{a_1^2+a_2^2}\sin\varphi\cos\varphi + \frac{b_{22}^a}{a_1^2+a_2^2}\cos^2\varphi\Big], \tag{3.15a}$$

$$\begin{aligned}\lambda_1 = \Big\{\Big[&\frac{m_2^a\cos\varphi}{(a_1^2+a_2^2)^{1/2}} - \frac{m_1^a\sin\varphi}{(a_1^2+a_2^2)^{1/2}} + \frac{b_{11}^a\sin 2\varphi}{2(a_1^2+a_2^2)} - \frac{(b_{12}^a+b_{21}^a)(2\cos^2\varphi-1)}{2(a_1^2+a_2^2)}\\ &- \frac{b_{22}^a\sin 2\varphi}{2(a_1^2+a_2^2)}\Big] + p\Big[-\frac{b_{11}^a}{a_1^2+a_2^2}\cos\varphi\sin\varphi\\ &+ \frac{b_{12}^a}{a_1^2+a_2^2}(\cos^2\varphi-\sin^2\varphi) + \frac{b_{22}^a}{a_1^2+a_2^2}\cos\varphi\sin\varphi\Big]\Big\},\end{aligned} \tag{3.15b}$$

$$\begin{aligned}\lambda_0 = p\Big\{&\frac{m_1^a}{(a_1^2+a_2^2)^{1/2}}\cos\varphi + \frac{m_2^a}{(a_1^2+a_2^2)^{1/2}}\sin\varphi\\ &+ \frac{1}{2}\Big[\frac{b_{11}^a}{a_1^2+a_2^2}[(p-2)\cos^2\varphi+1] + \frac{(b_{12}^a+b_{21}^a)}{2(a_1^2+a_2^2)}(p-2)\sin 2\varphi\\ &+ \frac{b_{22}^a}{a_1^2+a_2^2}[(p-2)\sin^2\varphi+1]\Big]\Big\}.\end{aligned} \tag{3.15c}$$

Substituting $a_1 = r\cos\varphi,\ \ a_2 = r\sin\varphi$ into Eq. (3.15), one may find that the coefficients λ_0, λ_1, and λ_2 are functions of φ and p only. Substituting Eqs. (B.2) and $a_1 = r\cos\varphi,\ \ a_2 = r\sin\varphi$ into Eq. (3.14) yields the eigenvalue problem, which will be simplified into Eq. (3.18) as follows. The moment Lyapunov exponents can then be calculated from this simplified eigenvalue problem.

To simplify the eigenvalue problem, the parameters ϖ_{11} and ϖ_{22} are deliberately chosen such that

$$\varpi_{21}^2 = \frac{\varpi_{22}^2}{\varpi_{11}^2} = \begin{cases} 1, & \text{if } \ D_1D_2 = 0,\\ \big(\frac{D_1}{D_2}\big)^{1/2}, & \text{if } \ D_1D_2 \neq 0.\end{cases}$$

From Eqs. (B.3) and (B.4), it is seen that D_1 and D_2 can be rewritten as

$$\begin{aligned}D_1 &= \Big(\upsilon_1 - \frac{1}{\upsilon_2}\Big)^2 S(\omega_1+\omega_2) + \Big(\upsilon_1 + \frac{1}{\upsilon_2}\Big)^2 S(\omega_1-\omega_2),\\ D_2 &= \Big(\upsilon_2 - \frac{1}{\upsilon_1}\Big)^2 S(\omega_1+\omega_2) + \Big(\upsilon_2 + \frac{1}{\upsilon_1}\Big)^2 S(\omega_1-\omega_2),\end{aligned}$$

which show that D_1 and D_2 are non-negative, and D_1 is zero if and only if D_2 equals zero.

Employing the notations

$$\begin{aligned}D = \varpi_{21}^2 D_2 = \varpi_{12}^2 D_1 = \sqrt{D_1D_2} &= \Big|\Big(\delta\upsilon_1\upsilon_2 + \frac{1}{\upsilon_1\upsilon_2}\Big)S^+ - 8S^-\Big|,\\ \tilde{a} = \frac{V_0}{4}(V_1+V_2-2V_3+2D), &\quad \tilde{b} = \frac{V_0}{4}(V_1+V_2-2V_3-2D),\\ \Delta_1 = E_1 + 2V_0(V_1+V_3), &\quad \Delta_2 = E_2 + 2V_0(V_2+V_3),\end{aligned} \tag{3.16}$$

where $V_i (i = 1,2,3,4)$, $E_i (i = 1,2)$ and $D_i (i = 1,2)$ are given in Eq. (B.3) of Appendix B, the eigenvalue problem becomes

$$\mathcal{L}(p) = (D - \tilde{b}\cos^2 2\varphi)T_{\varphi\varphi} + \Big\{p\Big[\frac{1}{2}V_0(V_2-V_1)\sin 2\varphi - \tilde{b}\sin 4\varphi\Big]$$

$$+\frac{1}{\sin 2\varphi}\Big[\frac{1}{2}(\Delta_2-\Delta_1)\sin^2(2\varphi)+2\cos 2\varphi(\tilde{a}-\tilde{b}\cos^2 2\varphi)\Big]\Big\}T_\varphi$$
$$+p\Big\{\frac{1}{2}(\Delta_1+\Delta_2)+\frac{1}{2}(\Delta_1-\Delta_2)\cos 2\varphi+2(D-\tilde{b}\cos^2 2\varphi)$$
$$+p(V_1\cos^2\varphi+V_2\sin^2\varphi+\tilde{b}\cos^2 2\varphi)\Big\}T=\Lambda T,\quad 0\leqslant\varphi<\pi.$$

The parameters $E_i(i=1,2)$ are called pseudo-damping coefficients.

3.2. Determination of moment Lyapunov exponents. It is found that the coefficients in Eq. (3.14) are periodic with period π. Therefore, it is reasonable to consider a Fourier cosine series (truncated at the K-th order) of the eigenfunction $T(\varphi)$ in the form

$$T^{(K)}(\varphi)=\sum_{i=0}^{K}C_i\cos(2i\varphi). \tag{3.17}$$

Here, only cosine functions are adopted because sometimes the eigenvalue problems in Eq. (3.14) contains $1/\sin(2\varphi)$.

Substituting Eq. (3.17) and $a_1=r\cos\varphi$, $a_2=r\sin\varphi$ into the eigenvalue problem (3.14), multiplying both sides by $\cos(2j\varphi)$, $j=0,1,\ldots,$ and performing integration with respect to φ from 0 to $\pi/2$, yield a set of $K+1$ equations for the unknown coefficients C_i, $i=0,1,\ldots,K$:

$$\sum_{i=0}^{K}a_{ij}C_i=\Lambda^{(K)}C_j,\quad j=0,1,2,\ldots,$$

or in the matrix form

$$\begin{bmatrix}a_{00}-\Lambda^{(K)} & a_{01} & \cdots & a_{0K}\\ a_{10} & a_{11}-\Lambda^{(K)} & \cdots & a_{1K}\\ \vdots & \vdots & \cdots & \vdots\\ a_{K0} & a_{K1} & \cdots & a_{KK}-\Lambda^{(K)}\end{bmatrix}\begin{Bmatrix}C_0\\C_1\\\vdots\\C_K\end{Bmatrix}=\mathbf{0}.$$

where $\Lambda^{(K)}$ denotes the kth-order approximate moment Lyapunov exponent and

$$a_{ij}=\frac{4}{\pi}\int_0^{\pi/2}\mathcal{L}(p)[\cos(2i\varphi)]\cos(2j\varphi)\mathrm{d}\varphi,\quad j=0,1,2,\ldots.$$

To obtain non-trivial solutions, the determinant is set to zero, yielding a polynomial equation of degree $K+1$ for the moment Lyapunov exponents $\Lambda^{(K)}(p)$,

$$e_{K+1}^{(K)}[\Lambda^{(K)}]^{K+1}+e_K^{(K)}[\Lambda^{(K)}]^K+\cdots+e_1^{(K)}\Lambda^{(K)}+e_0^{(K)}=0. \tag{3.18}$$

The set of approximate eigenvalues obtained through this procedure converges to the corresponding true eigenvalues as $K\to\infty$. However, as shown in Figure 1, the approximate eigenvalues converge so rapidly that the approximations nearly coincide for $K\geqslant 1$, i.e., $\Lambda_{\mathbf{q}(t)}(p)\approx\Lambda^{(K)}(p)$.

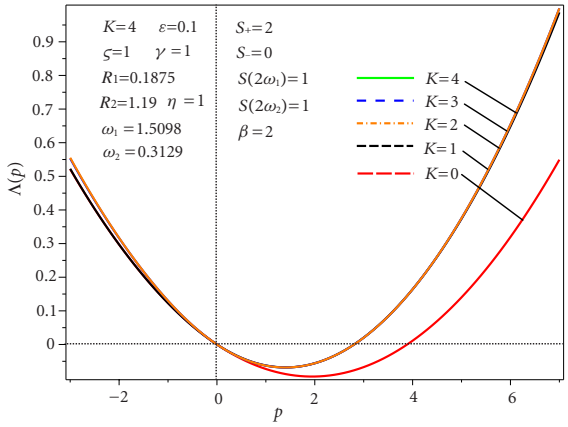

FIGURE 1. Moment Lyapunov exponents for various Kth order Fourier expansion

3.3. Determination of the largest Lyapunov exponents. The pth moment Lyapunov exponent $\Lambda_{\mathbf{q}(t)}(p)$ is a convex analytic function in p that passes through the origin, and the slope at the origin is equal to the largest Lyapunov exponent $\lambda_{\mathbf{q}(t)}$ [14],

$$\lambda_{\mathbf{q}(t)}(p) = \lim_{p\to 0} \frac{\Lambda_{\mathbf{q}(t)}(p)}{p}. \tag{3.19}$$

Eq. (2.6a) is similar to system Eq. (8.6.2) in the book [14], where the largest Lyapunov exponent was analytically derived from the invariant probability density by solving a Fokker–Plank equation [14]. The analytical results from [14], shown as dashed lines, and the numerical results from Eq. (3.19), shown as solid lines, are compared in Figure 2. The comparison indicates that the two sets of results are nearly indistinguishable and overlap. It should be noted, however, that due to round-off errors, the numerical results may become unstable as $S(\omega) \to 0$. Figure 2 also demonstrates that the analytical and numerical largest Lyapunov exponents closely approximate the tangent lines of the Monte Carlo simulations [33], shown as dotted lines. This serves as evidence that the stochastic averaging method is valid only as a first-order approximation.

3.4. Procedure for Stability analysis. The procedure for stochastic stability analysis is summarized as follows.

(1) Set up the governing equations of motion of a structure under stochastic loadings, e.g., Eq. (2.1). This is a Stratonovich stochastic differential equation.
(2) Express the state coordinates in polar coordinates, e.g., Eq. (2.4).
(3) Convert the Stratonovich stochastic differential equation into first-order differential equations in terms of amplitudes and phase angles, e.g., Eq. (2.5), based on the polar coordinates in Eq. (2.4).

(4) Apply stochastic averaging to approximate the first-order differential equations by averaged first-order differential equations in terms of averaged amplitudes and averaged phase angles, e.g., Eqs. (2.6a) and (2.6b), which are Itô stochastic differential equations.
(5) Apply Khasminskii's transformation in Eq. (3.1) together with the Itô lemma to obtain the Itô equations of the pth Euclidean norm, as in Eqs. (3.2) and (3.3).
(6) Use the linear stochastic transformation to obtain the eigenvalue problem in Eq. (3.12) or Eq. (3.13).
(7) Solve the eigenvalue problem using the Fourier cosine series in Eq. (3.17) to calculate the moment Lyapunov exponents in Eq. (3.18).
(8) Use the relationship between the largest Lyapunov exponent and the moment Lyapunov exponents in Eq. (3.19) to determine the largest Lyapunov exponent.

4. Stability Boundary

Although moment Lyapunov exponents can be determined numerically from Eq. (3.18), analytical expressions are sometimes needed. These can be obtained by setting $K = 0, 1, 2$ in Eq. (3.17) as follows.

4.1. For $K = 0$. When $K = 0$, the eigenfunction in Eq. (3.17) becomes $T(\varphi) = C_0$. Then, from $a_{00} - \Lambda^{(0)} = 0$, the moment Lyapunov exponent is given by

$$\Lambda_{\mathbf{q}(t)}(p) \approx \Lambda^{(0)}(p) = \frac{V_0}{8}(3V_1 + 3V_2 + 2V_3 + 2D)p^2 + \frac{1}{2}\left[\frac{V_0}{2}(5V_1 + 5V_2 + 6V_3 + 6D) - E_1 - E_2\right]p, \tag{4.1}$$

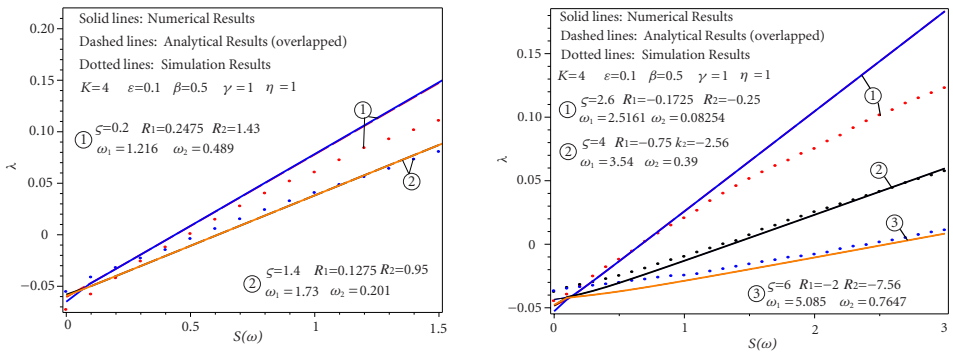

FIGURE 2. Comparisons of the largest Lyapunov exponents for analytical, numerical and simulation results

where $V_i (i = 1, 2, 3, 4)$ and $E_i (i = 1, 2)$ are given in Eq. (B.3) of Appendix B, but D is provided in Eq. (3.16). The system is moment stable if $\Lambda_{\mathbf{q}(t)}(p) < 0$, which gives the pth moment stability region for a given value of p.

The Lyapunov exponent is

$$\lambda^{(0)} = \lim_{p\to 0} \frac{\Lambda^{(0)}(p)}{p} = \frac{V_0}{4}(5V_1 + 5V_2 + 6V_3 + 6D) - \frac{1}{2}(E_1 + E_2). \tag{4.2}$$

The almost-sure stability region is given by $\lambda^{(0)} < 0$.

From Eqs. (4.1) and (4.2), both the moment stability boundary and the almost-sure and are straight lines in the coordinates defined by E_1 and E_2.

4.2. For $K = 1$. When $K = 1$, the eigenfunction is $T(\varphi) = C_0 + C_1 \cos 2\varphi$. The pth moment stability region is given by $\Lambda^{(1)} < 0$, in which $\Lambda^{(1)}$ are the roots of the quadratic equation

$$\left(\Lambda^{(1)}\right)^2 + e_1^{(1)}\Lambda^{(1)} + e_0^{(1)} = 0,$$

$$\left(\Lambda^{(1)}\right)^2 + \left[e_{12}^{(1)}p^2 + e_{11}^{(1)}p + e_{10}^{(1)}\right]\Lambda^{(1)} + \left[e_{04}^{(1)}p^4 + e_{03}^{(1)}p^3 + e_{02}^{(1)}p^2 + e_{01}^{(1)}p\right] = 0, \tag{4.3}$$

where

$$e_{12}^{(1)} = -\frac{1}{8}(13V_1 + 13V_2 + 6V_3 + 6D)V_0,$$

$$e_{11}^{(1)} = -\Big[\frac{1}{4}(21V_1 + 21V_2 + 22V_3 + 22D)V_0 + 2(E_1 + E_2)\Big],$$

$$e_{10}^{(1)} = (V_1 + V_2 - 2V_3 + 14D)V_0,$$

$$e_{04}^{(1)} = \Big[\frac{5}{64}(V_1^2 + V_2^2) + \frac{37}{32}V_1V_2 + \frac{5}{16}(V_3 + D)(V_1 + V_2) + \frac{1}{16}(V_3 + D)^2\Big]V_0^2,$$

$$\begin{aligned} e_{03}^{(1)} = \Big\{\Big[&\frac{5}{8}(V_1^2 + V_2^2) + \frac{29}{4}V_1V_2 + \frac{13}{4}(V_3 + D)(V_1 + V_2) + (V_3 + D)^2\Big]V_0 \\ &- \frac{3}{8}(E_1 + E_2)(D + V_3) - \Big(\frac{5}{16}E_1 + \frac{21}{16}E_2\Big)V_1 - \Big(\frac{5}{16}E_2 + \frac{21}{16}E_1\Big)V_2\Big\}V_0, \end{aligned}$$

$$\begin{aligned} e_{02}^{(1)} = \Big\{\Big[&\frac{1}{16}(V_1^2 + V_2^2) + \frac{97}{8}V_1V_2 + \Big(\frac{31}{4}V_3 + \frac{7}{4}D\Big)(V_1 + V_2) \\ &+ \frac{1}{4}(17V_3 + D)(V_3 + D)\Big]V_0^2 - \Big[\frac{11}{4}(E_1 + E_2)(D + V_3) \\ &+ \Big(\frac{5}{8}E_1 + \frac{37}{8}E_2\Big)V_1 + \Big(\frac{5}{8}E_2 + \frac{37}{8}E_1\Big)V_2\Big]V_0 + \frac{1}{4}E_1^2 + \frac{1}{4}E_2^2 + \frac{3}{2}E_1E_2\Big\}, \end{aligned}$$

$$\begin{aligned} e_{01}^{(1)} = \Big\{\Big[&-\frac{13}{4}(V_1^2 + V_2^2) + V_1V_3 + (\frac{3}{2}V_2 - 19D)V_1 + (V_3 - 19D)V_2 - 18DV_3 \\ &- 21D^2 + V_3^2\Big]V_0^2 + \Big[7(E_1 + E_2)D + \Big(\frac{5}{2}E_1 - \frac{3}{2}E_2\Big)V_1 \\ &+ \Big(\frac{5}{2}E_2 - \frac{3}{2}E_1\Big)V_2 - (E_1 + E_2)V_3\Big]V_0\Big\}, \end{aligned}$$

where $V_i (i = 1, 2, 3, 4)$ and $E_i (i = 1, 2)$ are given in Eq. (B.3) of Appendix B, but D is provided in Eq. (3.16). The Lyapunov exponent is given by

$$\lambda^{(1)} = -\lim_{p\to 0} \frac{e_{04}^{(1)} p^4 + e_{03}^{(1)} p^3 + e_{02}^{(1)} p^2 + e_{01}^{(1)} p}{p[e_{12}^{(1)} p^2 + e_{11}^{(1)} p + e_{10}^{(1)}]} = -\frac{e_{01}^{(1)}}{e_{10}^{(1)}}. \tag{4.4}$$

Analytical expressions for moment Lyapunov exponent $\Lambda^{(1)}$ can be obtained by solving quadratic equation Eq. (4.3). For clarity of presentation, the following special cases are considered.

Case 1: Gyroscopic systems under white noise excitation with $S(\omega) = S_0$. In this case, one has $S^+ = S_0$, $S^- = 0$, and

$$V_1 = \Big(\zeta\upsilon_1 - \frac{1}{\upsilon_1}\Big)^2 S_0, \quad V_2 = \Big(\zeta\upsilon_2 - \frac{1}{\upsilon_2}\Big)^2 S_0, \quad V_3 = 2\zeta S_0,$$
$$D_1 = \Big(\zeta^2\upsilon_1^2 + \frac{1}{\upsilon_2^2}\Big) S_0, \quad D_2 = \Big(\zeta^2\upsilon_2^2 + \frac{1}{\upsilon_1^2}\Big) S_0.$$

Case 2: Gyroscopic systems under band-limited noise excitation close to $S(2\omega_i)$, $i = 1, 2$.
Take $S(2\omega_1) = S_0$ as an example. In this case, one has $V_2 = V_3 = 0$ and $D_1 = D_2 = D = 0$. The moment Lyapunov exponent is given by

$$\begin{aligned}\Lambda^{(1)}(p) = {} & \frac{13}{32} V_0 V_1 p^2 + \Big[\frac{21}{16} V_0 V_1 - \frac{1}{2}(E_1 + E_2)\Big] p - \frac{1}{4} V_0 V_1 \\ & + \frac{1}{32}\big\{129 V_0^2 V_1^2 p^4 + [772 V_0^2 V_1^2 - 256(E_1 - E_2) V_0 V_1] p^3 \\ & + [1524 V_0^2 V_1^2 - 1024(E_1 - E_2) V_0 V_1 + 128(E_1 - E_2)^2] p^2 \\ & + [992 V_0^2 V_1^2 - 1024(E_1 - E_2) V_0 V_1 + 256(E_1 - E_2)^2] p\big\}^{1/2}.\end{aligned} \tag{4.5}$$

The corresponding largest Lyapunov exponent is

$$\lambda^{(1)}(p) = \frac{13}{4} V_0 V_1 - \frac{5}{2} E_1 + \frac{3}{2} E_2 + \frac{1}{2} \frac{(E_1 - E_2)^2}{V_0 V_1}. \tag{4.6}$$

The moment stability region and almost-sure stability region can be obtained from the equations $\Lambda^{(1)}(p) < 0$ and $\lambda^{(1)}(p) < 0$, respectively. Stability boundary is the dividing line between the stability region and the instability region. Therefore, from this boundary, one can establish the relation between E_1 and E_2, as well as the critical excitation S_0 for moment stability or almost-sure stability.

Case 3: Gyroscopic systems under band-limited noise excitation close to $S(\omega^+)$. In this case, from Eq. (B.3), one has $V_1 = V_2 = 0$, $S^+ = S^- = S(\omega^+)$, and

$$V_3 = \Big(2\zeta - \zeta^2\upsilon_1\upsilon_2 - \frac{1}{\upsilon_1\upsilon_2}\Big) S(\omega^+), \quad D_1 = \Big(\zeta^2\upsilon_1^2 + \frac{1}{\upsilon_2^2} - 2\frac{\zeta\upsilon_1}{\upsilon_2}\Big) S(\omega^+),$$
$$D_2 = \Big(\zeta^2\upsilon_2^2 + \frac{1}{\upsilon_1^2} - 2\frac{\zeta\upsilon_2}{\upsilon_1}\Big) S(\omega^+), \qquad D = \sqrt{D_1 D_2}.$$

The moment Lyapunov exponent is given by

$$\Lambda^{(1)}(p) = \frac{3}{16}V_0(V_3+D)p^2 + \Big[\frac{11}{8}V_0(V_3+D) - \frac{1}{2}(E_1+E_2)\Big]p - \Big(\frac{1}{2}V_3 - \frac{7}{2}D\Big)V_0 + \frac{1}{16}\big\{V_0^2(V_3+D)^2p^4 + 4V_0^2(V_3+D)^2p^3 + [(116D^2+104V_3^2D-12V_3^2)V_0^2 + 32(E_1-E_2)^2]p^2 + [(224D^2+192V_3D-32V_3^2)V_0^2 + 64(E_1-E_2)^2]p + (3136D^2-896V_3D+64V_3^2)V_0^2\big\}^{1/2}. \tag{4.7}$$

The corresponding largest Lyapunov exponent is

$$\lambda^{(1)}(p) = \frac{(42D^2+36V_3D-6V_3^2)V_0^2 + (E_1+E_2)(2V_3-14D)V_0 + (E_1-E_2)^2}{4(7D-V_3)V_0}.$$

Case 4: Gyroscopic systems under band-limited noise excitation close to $S(\omega^-)$. In this case, from Eq. (B.3), one has $V_1 = V_2 = 0$, $S^+ = -S^- = S(\omega^+)$, and

$$V_3 = \Big(2\zeta + \zeta^2\upsilon_1\upsilon_2 + \frac{1}{\upsilon_1\upsilon_2}\Big)S(\omega^-), \quad D_1 = \Big(\zeta^2\upsilon_1^2 + \frac{1}{\upsilon_2^2} + 2\frac{\zeta\upsilon_1}{\upsilon_2}\Big)S(\omega^-),$$
$$D_2 = \Big(\zeta^2\upsilon_2^2 + \frac{1}{\upsilon_1^2} + 2\frac{\zeta\upsilon_2}{\upsilon_1}\Big)S(\omega^-), \quad D = \sqrt{D_1D_2}.$$

The moment Lyapunov exponent and the corresponding largest Lyapunov exponents have the same form as Eq. (4.5) and (4.6), respectively.

The analytical expressions for the moment Lyapunov exponent and the Lyapunov exponent, given in Eq. (4.5) to (4.7), serve as invaluable tools for stability characterization with respect to variations in the spectral density. For example, by substituting Eq. (B.3) into Eq. (4.5) and setting $\Lambda^{(1)}(p) = 0$, one can determine the stability index and the stability boundary. Furthermore, if $\Lambda^{(1)}(p) < 0$, the corresponding stability region can be identified.

4.3. For $K = 2$. When $K = 2$, the eigenfunction takes the form $T(\varphi) = C_0 + C_1\cos 2\varphi + C_2\cos 4\varphi$, and the pth moment Lyapunov exponent $\Lambda^{(2)}$ is the root of a cubic equation. Although an explicit analytical result can be obtained, it too lengthy to be presented here. For $K \geqslant 3$, no explicit expressions for moment Lyapunov moments are available.

5. Application: Axially moving band

5.1. Equation of motion. The axially moving band of analysis is illustrated in Figure 3, where the flexural motion of a freely running band between two pulleys of equal radii R over a span, L. The band is modelled as an axially moving uniform beam with constant transport speed, ν, and is characterized by a mass per unit length, m, a flexural rigidity, $EI = EI_y$, and a material damping parameter, β.

Assumptions defining this problem are as follows.

(1) The bands are uniform, elastic Euler-Bernoulli beams.
(2) The coordinate axis, z, runs along the length of the band.
(3) Let u, w denote the lateral deflection of the band in the x, y directions, respectively. For a thin band (strip) the flexural rigidity $EI_y \ll EI_x$ and hence the in-plane deflection w may be neglected when compared to the lateral deflection u.

(4) The band tension consists of a static component and a dynamic component which includes the effects due to the centrifugal action, band-structure interaction, and a periodic fluctuation. The periodic fluctuation in tension is caused by pulley eccentricities or joints and flaws in the band.
(5) Slipping between the band and wheels does not occur.
(6) Out-of-plane motion of the spans does not occur.
(7) The longitudinal displacement of the spans are small compared to their transverse displacement.
(8) Dependent variable variations are significant only in the axial, x-direction.
(9) The dissipative forces in the transverse direction are considered to be due to aerodynamic forces and are taken to be proportional to the material velocities.
(10) The compliance of the band-structure is denoted by h. The compliance h may take values between 0 and 1 depending on the degree of band-support structure interaction. This factor is obtainable directly from static measurements or indirectly from the experimental frequency speed variation.

In the equilibrium configuration, the band is subjected to a static tension Γ_0 and it features a small initial curvature due to the bending of the band between the two rotating pulleys. The dynamic band tension $\Gamma(t)$ at constant axial transport speed is considered to consist of three components: a static component Γ_0, a velocity-dependent dynamic component, and a mean-zero random component $\varrho\mathfrak{f}(t)$, i.e.,

$$\Gamma(t) = \Gamma_0 - hm\nu^2 + \varrho\mathfrak{f}(t),$$

where $0 \leqslant h \leqslant 1$ is a compliance factor and ϱ is an amplitude scaling factor pertaining to the tension variation. $\mathfrak{f}(t)$ is the random tension fluctuation component and is assumed to be a stationary stochastic process with zero mean value. Experimental measurements of band tension confirms the presence of such a random component [34]. These factors are obtainable directly from static measurements or indirectly from the experimental frequency speed variation.

Under the above conditions, the equation of motion for the flexural vibration of the band for viscoelastic materials can be derived as [7, 34]

$$EI(1-\mathcal{H})\frac{\partial^4 u}{\partial z^4} + [mh\nu^2 - \Gamma_0 - \varrho\mathfrak{f}(t)]\frac{\partial^2 u}{\partial z^2} + \nu\beta\frac{\partial u}{\partial z} + 2\nu m\frac{\partial^2 u}{\partial z\partial t} + m\frac{\partial^2 u}{\partial t^2} + \beta\frac{\partial u}{\partial t} = 0, \tag{5.1}$$

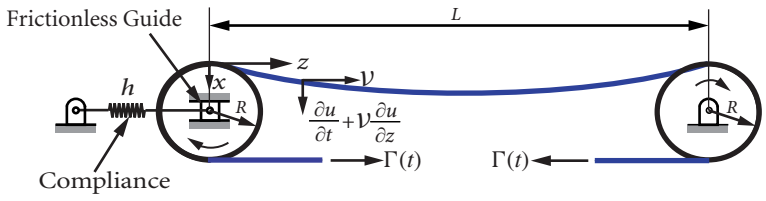

FIGURE 3. A schematic of the axially moving band-wheel systems

where $\mathcal{H}$ is a linear viscoelastic operator defined Eq. (2.2). The geometric boundary conditions are given by

$$u(0,t) = u(L,t) = 0, \quad \frac{\partial^2 u}{\partial z^2}\Big|_{(0,t)} = \frac{\partial^2 u}{\partial z^2}\Big|_{(L,t)} = 0.$$

It is noted that Eq. (5.1) is a partial differential equation, which is difficult to solve and so the Galerkin method is used in the following to convert it into ordinary differential equations by applying the method of separation of variables and assuming

$$u(z,t) = \sum_{i=1}^{\mathfrak{n}} q_i(t) \sin \frac{i\pi z}{L}, \tag{5.2}$$

where $q_i(t)$ is the generalized coordinates and the function $\sin \frac{i\pi z}{L}$ is mode shapes of a simply-supported beam of length L.

For simplicity, consider only the first two modes, i.e. $\mathfrak{n} = 2$. Substituting Eq. (5.2) into (5.1), multiplying both sides by $\sin \frac{i\pi z}{L}$, $i = 1, 2$, and integrating with respect to z from 0 to L yields

$$\begin{cases} q_1'' + \frac{\beta}{m} q_1' - \frac{16\nu}{3L} q_2' + \frac{EI\pi^4}{mL^4}[(1-\mathcal{H}) - \xi^*(t)]q_1 - \frac{8\nu\beta}{3mL} q_2 = 0, \\ q_2'' + \frac{\beta}{m} q_2' + \frac{16\nu}{3L} q_1' + \frac{EI(2\pi)^4}{mL^4}[(1-\mathcal{H}) - \frac{\xi^*(t)}{4}]q_2 + \frac{8\nu\beta}{3mL} q_1 = 0, \end{cases} \tag{5.3}$$

where

$$\xi^*(t) = \frac{L^2}{\pi^2 EI}[mh\nu^2 - \Gamma_0 - \varrho \mathfrak{f}(t)].$$

When the non-dimensional time τ is introduced as

$$\tau = \frac{\pi^2}{L^2}\sqrt{\frac{EI}{m}}t,$$

and the dot is used to denote differentiation with respect to the new time τ, Eq. (5.3) becomes

$$\begin{cases} \ddot{q}_1 + \varepsilon 2\beta \dot{q}_1 - \varsigma \dot{q}_2 - \varepsilon\mathcal{H}[q_1] + R_1 q_1 - \varepsilon\beta\varsigma q_2 + \varepsilon^{1/2}\xi(\tau) q_1 = 0, \\ \ddot{q}_2 + \varepsilon 2\beta \dot{q}_2 + \varsigma \dot{q}_1 - \varepsilon\mathcal{H}[q_2] + R_2 q_2 + \varepsilon\beta\varsigma q_1 + \varepsilon^{1/2} 4\xi(\tau) q_2 = 0, \end{cases} \tag{5.4}$$

or in matrix form

$$\ddot{\mathbf{q}} + \varepsilon 2\beta \dot{\mathbf{q}} + \varsigma \begin{bmatrix} 0 & -1 \\ 1 & 0 \end{bmatrix} \dot{\mathbf{q}} \begin{bmatrix} R_1 - \varepsilon\mathcal{H} & -\varepsilon\beta\varsigma \\ \varepsilon\beta\varsigma & R_2 - \varepsilon\mathcal{H} \end{bmatrix} \mathbf{q} + \varepsilon^{1/2} \begin{bmatrix} 1 & 0 \\ 0 & 4 \end{bmatrix} \xi(\tau)\mathbf{q} = \mathbf{0}, \tag{5.5}$$

where $\mathbf{q} = \{q_1, q_2\}^T$ and

$$R_1 = 1 - c_0\chi_0^2, \quad R_2 = 16 - 4c_0\chi_0^2, \quad c_0 = \frac{9\pi^2}{64}\Big(h - \frac{\Gamma_0}{m\nu^2}\Big),$$
$$\chi_0 = \frac{8\nu L}{3\pi^2}\sqrt{\frac{m}{EI}}, \quad \varsigma = 2\chi_0, \quad \beta = \frac{\beta L^2}{2\pi^2\sqrt{mEI}}, \quad \xi(\tau) = \frac{\varrho L^2}{\pi^2 EI}\mathfrak{f}(t).$$

The third term is a gyroscopic term. This represents a gyroscopic system under parametric excitations, where the damping and excitation are assumed to be small. Hence, a small parameter $0 < \varepsilon \ll 1$ is introduced. This equation has the same form as Eq. (2.1). It can also be shown that the equation of motion for torsional

vibration of the band has the same form as Eq. (5.5), with EI, replaced by the torsional rigidity GJ, but with warping rigidity neglected.

5.2. Moment stability and almost-sure stability. Moment Lyapunov exponents and the largest Lyapunov exponents can be obtained using the procedures outlined in Sections 3 and 4. Some stability boundaries are discussed here, while additional results are provided in Section 7, along with Monte Carlo simulations.

For gyroscopic systems under white noise excitations, the almost-sure stability boundaries are as illustrated in Figure 4. It is observed that the boundary line resulting from the first order expansion ($K = 0$) is tangent to the boundary curve derived from the second order expansion ($K = 1$). This indicates that the stability region obtained from the second-order expansion is significantly more restrictive than that from the first-order expansion.

For the case $K = 0$, the moment stability boundaries are generally narrower than the almost-sure stability boundaries. Moreover, as the parameter p increases, these moment stability boundaries become increasingly restrictive. However, this trend does not necessarily hold for $K = 1$, where it becomes difficult to clearly distinguish which boundary is more restrictive.

The critical power spectrum amplitude of the white noise excitation can be determined for the case $K = 0$ using Eqs. (4.1) and (4.2), and for the case $K = 1$ by solving the quadratic equation in Eq. (4.3) together with Eq. (4.4). So the critical excitation, defined as the power spectrum amplitude of the white/real noise excitation, serves as the threshold separating stability from instability. The results

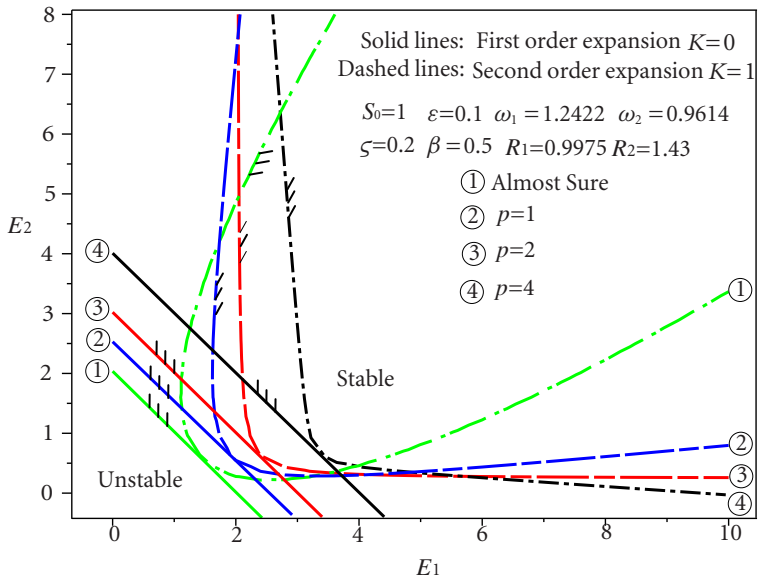

FIGURE 4. Almost-sure and pth moment stability boundaries under white noise

are illustrated in Figure 5, and selected numerical values corresponding to discrete points in the figure are listed in Tables 1 and 2 for reference.

It is observed that the critical excitation increases with the pseudo-damping coefficient E_1, confirming that damping and viscoelasticity absorb part of the vibration energy, thereby enhancing stability. For the case $K = 0$, the stability region associated with higher-order moments is more restrictive than those corresponding to lower-order moment stability and almost-sure stability. However, this trend does not appear to persist for the case $K = 1$.

A similarity is observed between the almost-sure and p-th moment stability boundaries under white noise excitations, as shown in Figure 4, and those under real noise excitations, depicted in Figure 6, aside from differences in their quantitative values. However, the behavior of critical excitation amplitudes differs significantly between systems subjected to white noise (Figure 5) and those subjected to real noise (Figure 7). Unlike the white noise case, where the critical excitation amplitude

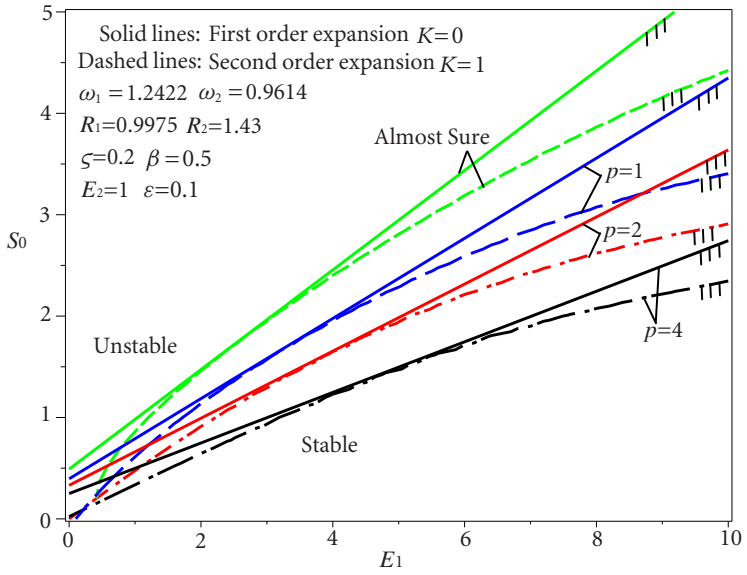

FIGURE 5. Critical excitation and pseudo-damping under white noise

TABLE 1. Critical excitations S_0 for case $K = 0$ under white noise

E_1	$p = 0$	$p = 1$	$p = 2$	$p = 4$
0	0.4910	0.3953	0.3308	0.2494
2	1.4731	1.1859	0.9924	0.7483
4	2.4551	1.9765	1.6541	1.2472
6	3.4372	2.7672	2.3157	1.7461
8	4.4193	3.5578	2.9774	2.2449

TABLE 2. Critical excitations S_0 for case $K = 1$ under white noises

E_1	$p = 0$	$p = 1$	$p = 2$	$p = 4$
0	0	0	0	0.0226
2	1.4626	1.1397	0.9130	0.6451
4	2.4031	1.9618	1.6537	1.2325
6	3.1908	2.5951	2.2152	1.7273
8	3.8680	3.0784	2.6217	2.0805

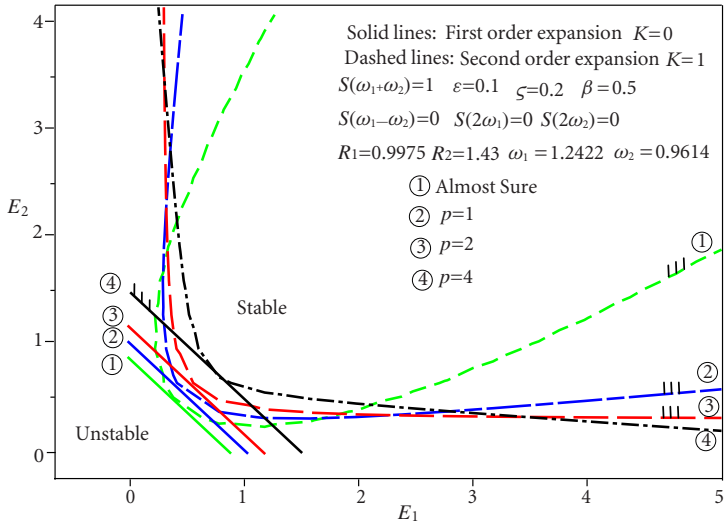

FIGURE 6. Almost-sure and pth moment stability boundaries under real noise

generally increases with the pseudo-damping coefficient, the system under real noise does not follow this trend consistently. In particular, for almost-sure stability, the critical power spectrum amplitude due to real noise may form an elliptical boundary.

5.3. Stability index. The stability index is defined as the non-trivial zero of the moment Lyapunov exponent and serves as a key parameter in characterizing the stability range of moment stability. The larger the value of the stability index, the more stable of the system in the sense of moment stability. It can be determined by solving a root-finding problem of the form $\Lambda_{\mathbf{q}(t)}(\delta_{\mathbf{q}(t)}) = 0$ [14]. In the case of white noise excitation, when the Fourier expansion order is $K = 0$, the stability index can be explicitly obtained from Eq. (4.1) and is given by

$$\delta_{q(t)} = \frac{\frac{V_0}{4}(3V_1 + 3V_2 + 2V_3 + 2\beta)}{\frac{V_0}{2}(5V_1 + 5V_2 + 6V_3 + 6\beta) - E_1 - E_2}.$$

When $K = 1$, the stability index corresponds to the non-trivial root of Eq. (4.7), which is generally not expressible in closed form. Representative results for the

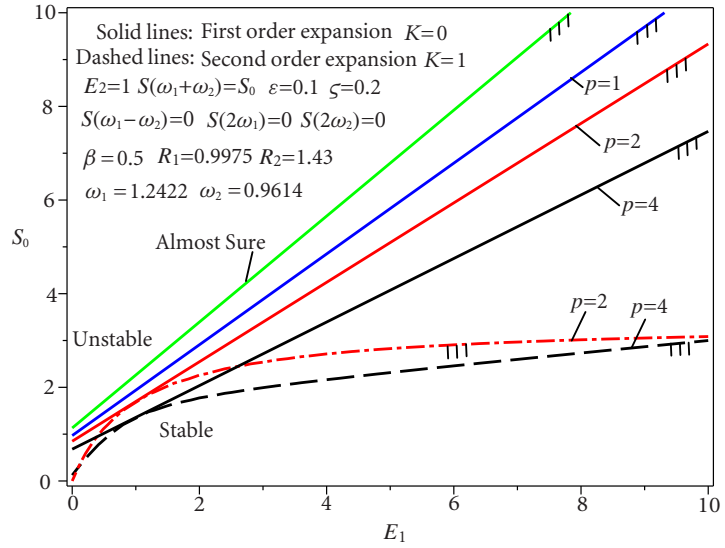

FIGURE 7. Critical excitation and pseudo-damping under real noise

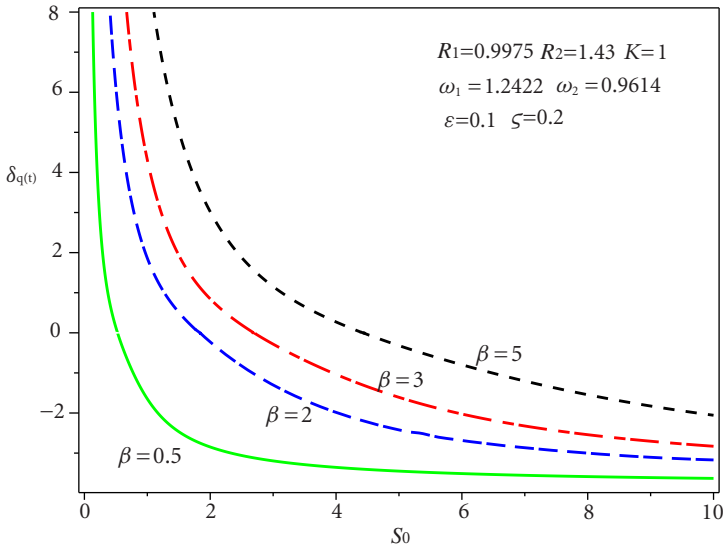

FIGURE 8. Stability index for a system under white noise

stability index are illustrated in Figure 8. It is observed that the stability index decreases from positive to negative values as the amplitude of the power spectrum increases, indicating that stronger noise destabilizes the system. Additionally, a larger damping coefficient β leads to a higher stability index, implying enhanced stability. Similar trends are found for systems under real noise excitation, as shown in Figure 9.

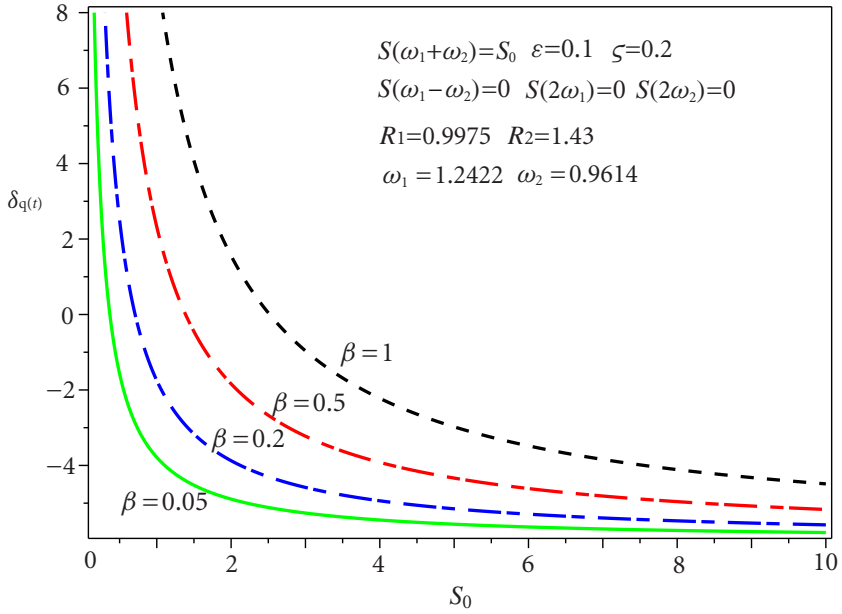

FIGURE 9. Stability index for a system under real noise

6. Simulation

In this section, Monte Carlo simulations are employed to evaluate the pth moment Lyapunov exponents and to verify the accuracy of the approximate results obtained via stochastic averaging. The analysis is based on the 2DOF system with a viscoelastic model described in Eq. (5.4). Two different models of wide-band noise excitation are considered separately: Gaussian white noise and Ornstein–Uhlenbeck (real) noise.

6.1. Gaussian white noise. In this case, the wide-band noise is modeled as Gaussian white noise. The excitation is approximated by a Gaussian white noise process with a flat spectral density, $S(\omega) = \vartheta^2$, constant for all ω. Thus, the stochastic process can be represented as $\xi(t)\mathrm{d}t = \vartheta\,\mathrm{d}W(t)$, where $W(t)$ denotes the standard Wiener process. Define the state variables as follows:

$$x_1(t) = q_1(t), \quad x_2(t) = \dot{q}_1(t), \quad x_3(t) = q_2(t), \quad x_4(t) = \dot{q}_2(t),$$
$$x_5(t) = \int_0^t \gamma e^{-\kappa(t-s)} q_1(s)\mathrm{d}s, \quad x_6(t) = \int_0^t \gamma e^{-\kappa(t-s)} q_2(s)\mathrm{d}s,$$

where $x_5(t)$ and $x_6(t)$ are related to viscoelasticity.

With this formulation, Eq. (5.4) is transformed into a six-dimensional system of Itô differential equations

$$\mathrm{d}\mathbf{x} = \mathbf{A}\mathbf{x}\,\mathrm{d}t + \mathbf{B}\mathbf{x}\vartheta\,\mathrm{d}W, \tag{6.1}$$

where $\mathbf{x} = \{x_1, x_2, x_3, x_4, x_5, x_6\}^T$, and the system matrices $\mathbf{A}$ and $\mathbf{B}$ are defined as:

$$\mathbf{A} = \begin{bmatrix} 0 & 1 & 0 & 0 & 0 & 0 \\ -R_1 & -\varepsilon 2\beta & \varepsilon\beta\varsigma & \varsigma & \varepsilon & 0 \\ 0 & 0 & 0 & 1 & 0 & 0 \\ -\varepsilon\beta\varsigma & -\varsigma & -R_2 & -\varepsilon 2\beta & 0 & \varepsilon \\ \gamma & 0 & 0 & 0 & -\kappa & 0 \\ 0 & 0 & \gamma & 0 & 0 & -\kappa \end{bmatrix}, \quad \mathbf{B} = \begin{bmatrix} 0 & 0 & 0 & 0 & 0 & 0 \\ -\varepsilon^{1/2} & 0 & 0 & 0 & 0 & 0 \\ 0 & 0 & 0 & 0 & 0 & 0 \\ 0 & 0 & -4\varepsilon^{1/2} & 0 & 0 & 0 \\ 0 & 0 & 0 & 0 & 0 & 0 \\ 0 & 0 & 0 & 0 & 0 & 0 \end{bmatrix}.$$

Eq. (6.1) represents a linear homogeneous stochastic differential system. To compute the moment Lyapunov exponents, the algorithm introduced by Xie [14] is employed. The norm used in the evaluation is defined by $\|\mathbf{x}(t)\| = \sqrt{\sum_{i=1}^{6} x_i^2}$. The system is numerically integrated using the explicit Euler scheme, with the iterative update equations given by:

$$\begin{aligned}
x_1^{k+1} &= x_1^k + x_2^k \cdot \Delta t, \\
x_2^{k+1} &= x_2^k + [-R_1 x_1^k - \varepsilon 2\beta x_2^k + \varepsilon\beta\varsigma x_3^k + \varsigma x_4^k + \varepsilon x_5^k]\Delta t - \varepsilon^{1/2} x_1^k \vartheta \cdot \Delta W^k, \\
x_3^{k+1} &= x_3^k + x_4^k \cdot \Delta t, \\
x_4^{k+1} &= x_4^k + [-\varepsilon\beta\varsigma x_1^k - \varsigma x_2^k - R_2 x_3^k - \varepsilon 2\beta x_4^k + \varepsilon x_6^k]\Delta t - 4\varepsilon^{1/2} x_3^k \vartheta \cdot \Delta W^k, \\
x_5^{k+1} &= x_5^k + \big(\gamma x_1^k - \kappa x_5^k\big)\Delta t, \\
x_6^{k+1} &= x_6^k + \big(\gamma x_3^k - \kappa x_6^k\big)\Delta t,
\end{aligned}$$

where Δt is the time step size and k denotes the kth iteration.

6.2. Ornstein–Uhlenbeck (real) noise. Denote

$$x_1(t) = q_1(t), \quad x_2(t) = \dot{q}_1(t), \quad x_3(t) = q_2(t), \quad x_4(t) = \dot{q}_2(t),$$

$$x_5(t) = \int_0^t \gamma e^{-\kappa(t-s)} q_1(s)\mathrm{d}s, \quad x_6(t) = \int_0^t \gamma e^{-\kappa(t-s)} q_2(s)\mathrm{d}s, \quad x_7(t) = \xi(t),$$

where $x_5(t)$ and $x_6(t)$ are related to viscoelasticity. $x_7(t)$ is the real noise.

Eq. (5.4) can be converted into the Itô differential equation:

$$\mathrm{d}\mathbf{x} = \mathbf{A}\mathbf{x}\,\mathrm{d}t + \mathbf{B}\,\mathrm{d}!W,$$

where $\mathbf{x} = \{x_1, x_2, x_3, x_4, x_5, x_6, x_7\}^T$, and

$$\mathbf{A} = \begin{bmatrix} 0 & 1 & 0 & 0 & 0 & 0 & 0 \\ -R_1 & -\varepsilon 2\beta & \varepsilon\beta\varsigma & \varsigma & \varepsilon & 0 & -\varepsilon^{1/2} x_1 \\ 0 & 0 & 0 & 1 & 0 & 0 & 0 \\ -\varepsilon\beta\varsigma & -\varsigma & -R_2 & -\varepsilon 2\beta & 0 & \varepsilon & -4\varepsilon^{1/2} x_3 \\ \gamma & 0 & 0 & 0 & -\kappa & 0 & 0 \\ 0 & 0 & \gamma & 0 & 0 & -\kappa & 0 \\ 0 & 0 & 0 & 0 & 0 & 0 & -\alpha \end{bmatrix}, \quad \mathbf{B} = \begin{bmatrix} 0 \\ 0 \\ 0 \\ 0 \\ 0 \\ 0 \\ \vartheta \end{bmatrix}.$$

The norm used for evaluating the moment Lyapunov exponents is defined as $\|\mathbf{x}(t)\| = \sqrt{\sum_{i=1}^{6} x_i^2}$. The discretized equations using the explicit Euler scheme are

$$
\begin{aligned}
x_1^{k+1} &= x_1^k + x_2^k \cdot \Delta t,\\
x_2^{k+1} &= x_2^k + [-R_1 x_1^k - \varepsilon 2\beta x_2^k + \varepsilon\beta\varsigma x_3^k + \varsigma x_4^k + \varepsilon x_5^k - \varepsilon^{1/2} x_1^k x_7^k]\Delta t,\\
x_3^{k+1} &= x_3^k + x_4^k \cdot \Delta t,\\
x_4^{k+1} &= x_4^k + [-\varepsilon\beta\varsigma x_1^k - \varsigma x_2^k - R_2 x_3^k - \varepsilon 2\beta x_4^k + \varepsilon x_6^k - 4\varepsilon^{1/2} x_3^k x_7^k]\Delta t,\\
x_5^{k+1} &= x_5^k + \left(\gamma x_1^k - \kappa x_5^k\right)\Delta t,\\
x_6^{k+1} &= x_6^k + \left(\gamma x_3^k - \kappa x_6^k\right)\Delta t,\\
x_7^{k+1} &= x_7^k + \left(-\alpha x_7^k\right)\cdot \Delta t + \sigma \cdot \Delta W^k,
\end{aligned}
$$

where Δt is the time step size and k denotes the kth iteration.

In the Monte Carlo Simulation, the number of iterations is 10^8, the time step is $\Delta t = 0.0005$, and the sample size is $N = 5000$.

7. Results and discussions

Figure 10 shows that as the damping coefficient β increases, the slope of the moment curves at the origin changes from negative to positive, indicating a transition from instability to stability. This suggests that damping plays a stabilizing role in the flexural-torsional behavior of the beam under both white noise and real noise excitation.

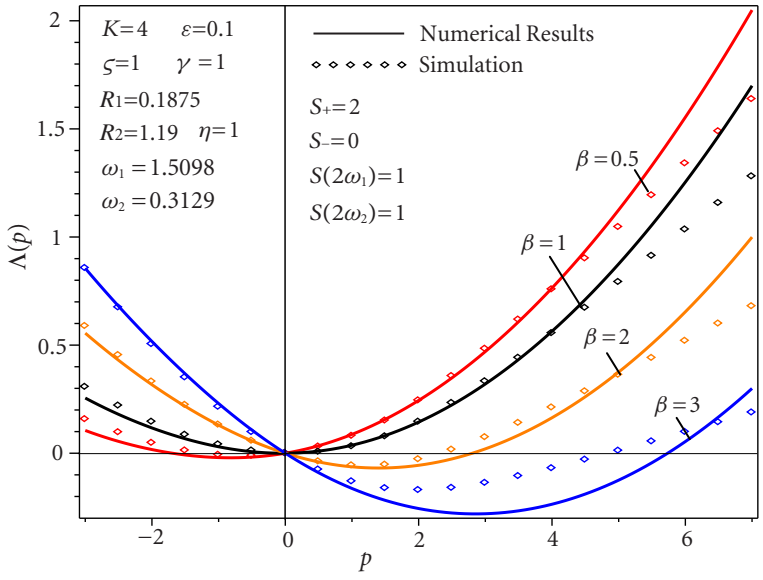

FIGURE 10. Effect of damping on Moment Lyapunov exponents under white noise

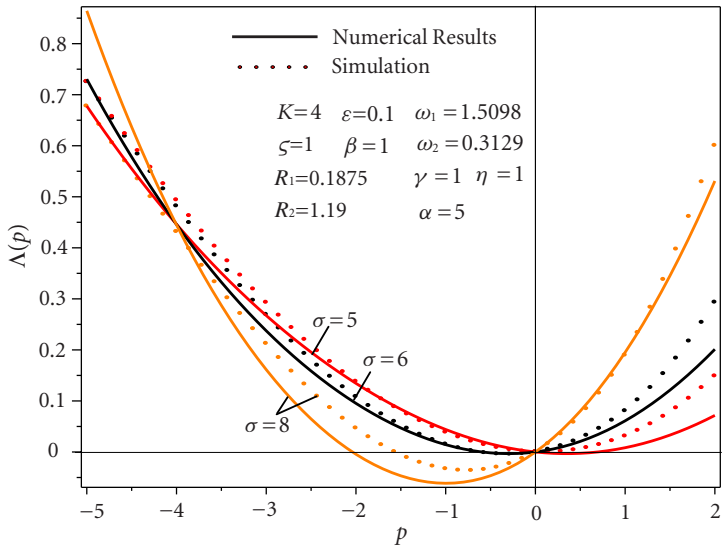

FIGURE 11. Effect of σ on Moment Lyapunov exponents under real noise

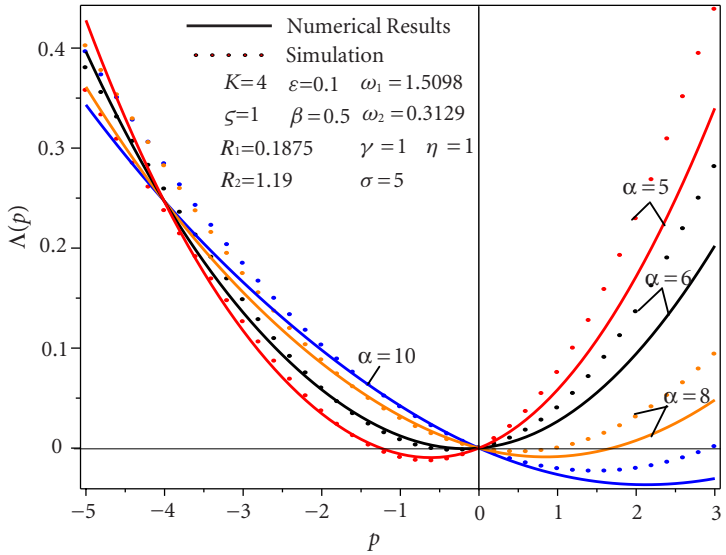

FIGURE 12. Effect of α on Moment Lyapunov exponents under real noise

Figures 11 and 12 illustrate the variation of moment Lyapunov exponents with respect to the parameters of real noise. A larger noise parameter σ narrows the stability region for $p > 0$, making the system more unstable. In contrast, the parameter α has a stabilizing effect: as α increases, the stability region for the pth

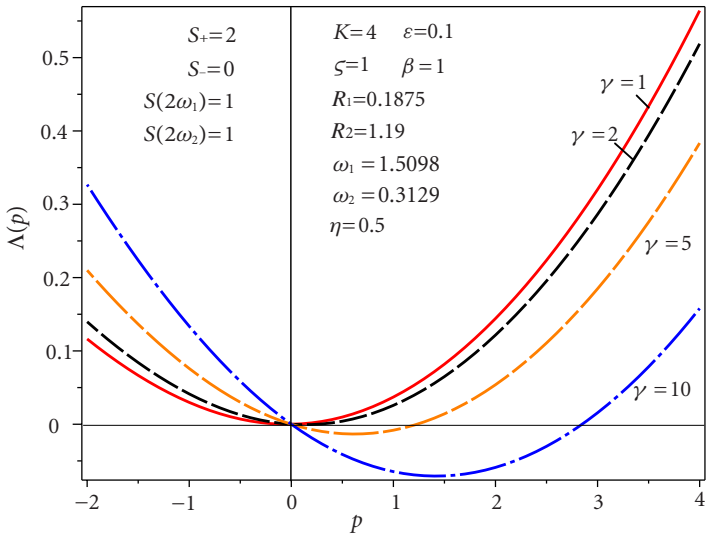

FIGURE 13. Effect of viscosity γ on Moment Lyapunov exponents under white noise

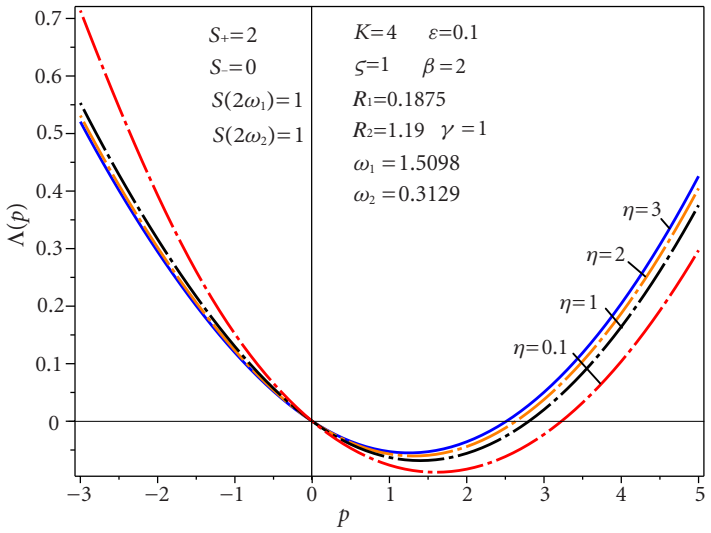

FIGURE 14. Effect of viscosity ρ on Moment Lyapunov exponents under white noise

moment (for $p > 0$) expands, resulting in a more stable system. This can be explained using Eq. (2.3), which indicates that a smaller σ or larger α reduces the power of the cosine spectral density. Consequently, the noise power is distributed over a wider frequency band, thereby reducing the power near resonance and enhancing system stability.

As shown in the figures, the simulation results agree well with the analytical approximations, demonstrating that the stochastic averaging method is effective for stability analysis of gyroscopic systems.

The ordinary Maxwell viscoelastic material in Eq. (B.8) also plays significant role in the stability of the gyroscopic system. As shown in Figure 13, the viscoelastic intensity γ has a stabilizing effect, but the relaxation rate η exerts a destabilizing influence under white-noise excitation, as illustrated in Figure 14. Increasing γ widens the stability region for $p > 0$, indicating its beneficial contribution to system stabilization; its stabilizing influence is generally more pronounced than the destabilizing effect of η. The destabilizing impact of η is notable only when η is small. A decrease in η corresponds to a longer relaxation time, which also widens the stability region for $p > 0$, showing that a larger relaxation time promotes system stability. These observations can be extended to systems subjected to real noise.

8. Conclusions

The stochastic stability of gyroscopic viscoelastic systems described by Stratonovich stochastic integro-differential equations was investigated. The system was parametrically excited by wide-band noise of small intensity, and small damping was assumed. The Stratonovich equations of motion were first decoupled into two-dimensional Itô stochastic differential equations using the method of stochastic averaging for the non-viscoelastic terms and the Larionov method for the viscoelastic terms. An elegant scheme for determining the moment Lyapunov exponents is presented, relying on stochastic transformations applied to the decoupled Itô equations. The resulting moment Lyapunov exponents and the largest Lyapunov exponents show good agreement with Monte Carlo simulation results and other analytical expressions from literature.

As an application, the stability of an axially moving band under stochastically fluctuating tension is examined. The stability region obtained from the second-order expansion is significantly more restrictive than that from the first-order expansion. It is found that, under wide-band noise excitation, the damping parameter β, the viscoelastic intensity γ, and the real noise band-width parameter α have stabilizing effects on both moment and almost-sure stability. However, the real noise intensity σ and the relaxation rate η have destabilizing effects. These findings provide new insights for engineering applications of gyroscopic viscoelastic systems. This paper focuses on the theoretical development and numerical validation. Experimental investigation is an important direction for the future research.

Acknowledgement. The research for this paper was supported, in part, by the Natural Sciences and Engineering Research Council of Canada.

Appendix A. Equations of motion in polar coordinates

This Appendix describes the process of transforming the equations of motion for a two degrees-of-freedom gyroscopic system in Eq. (2.1) from generalized coordinates $q_i(t)$ and their velocities $\dot{q}_i(t)$ into equations with polar coordinates in terms of amplitude and phase angles in Eq. (A.16) or Eq. (2.5). Although Eq. (2.1) is a

second-order differential equation and (A.16) is a first-order differential equation, all are Stratonovich differential equations. The transformation to polar coordinates is a necessary step for applying the stochastic averaging method, as referenced in [14]. The Stratonovich differential equations with polar coordinates will be averaged to Itô differential equations with polar coordinates in Appendix B.

Consider the unperturbed system of Eq. (2.1), i.e., $\varepsilon = 0$ and $\xi(t) = 0$, which takes the form:

$$\ddot{q}_1 + k_1 q_1 - \varsigma \dot{q}_2 = 0, \quad \ddot{q}_2 + k_2 q_2 + \varsigma \dot{q}_1 = 0. \tag{A.1}$$

This is a system of two linear second-order ordinary differential equations, which can be solved using the method of operators [35]. By introducing the D-operator, defined as $\mathrm{D}(\cdot) = \mathrm{d}(\cdot)/\mathrm{d}t$, the system becomes:

$$(\mathrm{D}^2 + k_1)q_1 - \varsigma \mathrm{D} q_2 = 0, \quad \varsigma \mathrm{D} q_1 + (\mathrm{D}^2 + k_2)q_2 = 0.$$

The determinant of the coefficient matrix is

$$\phi(\mathrm{D}) = \begin{vmatrix} \mathrm{D}^2 + k_1 & -\varsigma \mathrm{D} \\ \varsigma \mathrm{D} & \mathrm{D}^2 + k_2 \end{vmatrix}. \tag{A.2}$$

The corresponding characteristic equation of Eq. (A.2) is $\phi(\lambda) = \lambda^4 + (k_1 + k_2 + \varsigma^2)\lambda^2 + k_1 k_2 = 0$. This is a quadratic equation in λ^2,the solutions of which are

$$\lambda_{1,2}^2 = \frac{-(k_1 + k_2 + \varsigma^2) \mp \sqrt{(k_1 + k_2 + \varsigma^2)^2 - 4k_1 k_2}}{2}. \tag{A.3}$$

with $\lambda_1^2 < \lambda_2^2$. Denoting $\lambda_{1,2}^2 = -\omega_{1,2}^2$, Eq. (A.3) becomes

$$\omega_{1,2}^2 = \frac{(k_1 + k_2 + \varsigma^2) \pm \sqrt{(k_1 + k_2 + \varsigma^2)^2 - 4k_1 k_2}}{2}. \tag{A.4}$$

To ensure that the undamped and unperturbed system is stable, the eigenfrequencies $\omega_{1,2}$ must be real. The conditions for this are:

$$(k_1 + k_2 + \varsigma^2)^2 - 4k_1 k_2 > 0, \quad k_1 k_2 > 0.$$

It can be easily shown that

$$\frac{\omega_i^2 - k_1}{\varsigma \omega_i} = \frac{\varsigma \omega_i}{\omega_i^2 - k_2} = \upsilon_i, \quad i = 1, 2. \tag{A.5}$$

The complementary solutions for q_1 and q_2 in Eq. (A.1) have the same form and are given by

$$\begin{cases} q_1 = A_{11} \cos \omega_1 t + A_{12} \sin \omega_1 t + A_{13} \cos \omega_2 t + A_{14} \sin \omega_2 t, \\ q_2 = A_{21} \cos \omega_1 t + A_{22} \sin \omega_1 t + A_{23} \cos \omega_2 t + A_{24} \sin \omega_2 t, \end{cases} \tag{A.6}$$

which contain eight arbitrary constants. However, since $\phi(\mathrm{D})$ is a polynomial of degree 4 in D, the complementary solutions should contain only four arbitrary constants [35]. The four extra constants can be eliminated by substituting Eq. (A.6) into the first equation (A.1). Hence, the complementary solutions can be written as

$$q_1 = \varpi_{11} a_1 \sin \Phi_1 + \varpi_{22} a_2 \sin \Phi_2, \quad q_2 = \varpi_{11} a_1 \upsilon_1 \cos \Phi_1 + \varpi_{22} a_2 \upsilon_2 \cos \Phi_2,$$

where $\Phi_1 = \omega_1 t + \phi_1$ and $\Phi_2 = \omega_2 t + \phi_2$. The four constants are a_1, a_2, ϕ_1, and ϕ_2, while the other two coefficients, ϖ_{11} and ϖ_{22}, are suitable coordinate scaling parameters to make the evaluation of the moment Lyapunov exponent somewhat simpler.

Now, the method of variation of parameters is used to determine the solutions of the original perturbed system. First, differentiate q_1 and q_2 with respect to t to obtain equations for $\dot{q}_1$ and $\dot{q}_2$, and then vary the parameters a_1, a_2, ϕ_1, and ϕ_2 in equations for q_1, q_2, $\dot{q}_1$, and $\dot{q}_2$ to make them functions of t. This leads to solutions of the form

$$\begin{cases} q_1 = \varpi_{11} a_1(t) \sin\Phi_1 + \varpi_{22} a_2(t) \sin\Phi_2, \\ q_2 = \varpi_{11} a_1(t) \upsilon_1 \cos\Phi_1 + \varpi_{22} a_2(t) \upsilon_2 \cos\Phi_2. \end{cases} \tag{A.7}$$

$$\begin{cases} \dot{q}_1 = \varpi_{11} a_1(t) \omega_1 \cos\Phi_1 + \varpi_{22} a_2(t) \omega_2 \cos\Phi_2, \\ \dot{q}_2 = -\varpi_{11} a_1(t) \omega_1 \upsilon_1 \sin\Phi_1 - \varpi_{22} a_2(t) \omega_2 \upsilon_2 \sin\Phi_2. \end{cases} \tag{A.8}$$

Differentiating q_1 and q_2 in Eq. (A.7) and comparing the resulting equations with $\dot{q}_1$ and $\dot{q}_2$ in Eq. (A.8) gives

$$\begin{cases} \varpi_{11}\dot{a}_1 \sin\Phi_1 + \varpi_{11} a_1 \dot{\phi}_1 \cos\Phi_1 + \varpi_{22}\dot{a}_2 \sin\Phi_2 + \varpi_{22} a_2 \dot{\phi}_2 \cos\Phi_2 = 0, \\ \upsilon_1 \varpi_{11}\dot{a}_1 \cos\Phi_1 - \upsilon_1 \varpi_{11} a_1 \dot{\phi}_1 \sin\Phi_1 + \upsilon_2 \varpi_{22}\dot{a}_2 \cos\Phi_2 - \upsilon_2 \varpi_{22} a_2 \dot{\phi}_2 \sin\Phi_2 = 0. \end{cases} \tag{A.9}$$

Taking derivatives of $\dot{q}_1$ and $\dot{q}_2$ in Eq. (A.8) gives equations for $\ddot{q}_1$ and $\ddot{q}_2$. Substituting these $\ddot{q}_1$ and $\ddot{q}_2$, q_1 and q_2 in Eq. (A.7), and $\dot{q}_1$ and $\dot{q}_2$ in Eq. (A.8) into Eq. (2.1) yields

$$\begin{aligned} &\varpi_{11}\dot{a}_1\omega_1 \cos\Phi_1 - \varpi_{11} a_1 \omega_1 (\omega_1 + \dot{\phi}_1) \sin\Phi_1 + \varpi_{22}\dot{a}_2\omega_2 \cos\Phi_2 \\ &\quad - \varpi_{22} a_2 \omega_2 (\omega_2 + \dot{\phi}_2) \sin\Phi_2 + k_1[\varpi_{11} a_1 \sin\Phi_1 + \varpi_{22} a_2 \sin\Phi_2] \\ &\qquad + \varsigma[\varpi_{11}\upsilon_1\omega_1 a_1 \sin\Phi_1 + \varpi_{22}\upsilon_2\omega_2 a_2 \sin\Phi_2] - F = 0, \end{aligned} \tag{A.10}$$

$$\begin{aligned} &-\varpi_{11}\upsilon_1\dot{a}_1\omega_1 \sin\Phi_1 - \varpi_{11}\upsilon_1 a_1 \omega_1 (\omega_1 + \dot{\phi}_1) \cos\Phi_1 - \varpi_{22}\upsilon_2\dot{a}_2\omega_2 \sin\Phi_2 \\ &\quad - \varpi_{22}\upsilon_2 a_2 \omega_2 (\omega_2 + \dot{\phi}_2) \cos\Phi_2 + k_2[\varpi_{11}\upsilon_1 a_1 \cos\Phi_1 + \varpi_{22}\upsilon_2 a_2 \cos\Phi_2] \\ &\qquad + \varsigma[\varpi_{11}\omega_1 a_1 \cos\Phi_1 + \varpi_{22}\omega_2 a_2 \cos\Phi_2] - G = 0, \end{aligned} \tag{A.11}$$

where

$$\begin{aligned} F &= -\varepsilon[-\mathcal{H}[q_1] + 2\beta_a \dot{q}_1 - \beta_b \varsigma q_2] - \varepsilon^{1/2}\xi(t) q_1, \\ G &= -\varepsilon[-\delta\mathcal{H}[q_2] + 2\beta_a \dot{q}_2 + \beta_b \varsigma q_1] - \varepsilon^{1/2}\zeta\xi(t) q_2. \end{aligned} \tag{A.12}$$

Applying $\upsilon_i = (\omega_i^2 - k_1)/(\varsigma\omega_i)$ to Eq. (A.10), and $\upsilon_i = (\varsigma\omega_i)/(\omega_i^2 - k_2)$, $i = 1, 2$, to (A.11) leads to

$$\begin{aligned} &\varpi_{11}\dot{a}_1\omega_1 \cos\Phi_1 - \varpi_{11} a_1 \omega_1 \dot{\phi}_1 \sin\Phi_1 + \varpi_{22}\dot{a}_2\omega_2 \cos\Phi_2 - \varpi_{22} a_2 \omega_2 \dot{\phi}_2 \sin\Phi_2 - F = 0, \\ &-\varpi_{11}\upsilon_1\omega_1(\dot{a}_1 \sin\Phi_1 + a_1\dot{\phi}_1 \cos\Phi_1) - \varpi_{22}\upsilon_2\omega_2(\dot{a}_2 \sin\Phi_2 + a_2\dot{\phi}_2 \cos\Phi_2) - G = 0. \end{aligned} \tag{A.13}$$

Solving Eqs. (A.9) and (A.13) leads to a system of four first-order equations in terms of $\dot{a}_i$ and $a_i\dot{\phi}_i$, $i = 1, 2$,

$$\text{(A.14)}\quad \begin{cases} \dot{a}_1 = \frac{A}{\varpi_{11}}(+B_1 F\cos\Phi_1 - G\sin\Phi_1), & a_1\dot{\phi}_1 = \frac{A}{\varpi_{11}}(-B_1 F\sin\Phi_1 - G\cos\Phi_1), \\ \dot{a}_2 = \frac{A}{\varpi_{22}}(-B_2 F\cos\Phi_2 + G\sin\Phi_2), & a_2\dot{\phi}_2 = \frac{A}{\varpi_{22}}(+B_2 F\sin\Phi_2 + G\cos\Phi_2), \end{cases}$$

where

$$\text{(A.15)}\quad A = \frac{1}{\upsilon_1\omega_1 - \upsilon_2\omega_2} = \frac{\varsigma}{\omega_1^2 - \omega_2^2},$$

$$B_1 = -\frac{\upsilon_2(\upsilon_1\omega_1 - \upsilon_2\omega_2)}{\upsilon_1\omega_2 - \upsilon_2\omega_1} = -\frac{\upsilon_2\omega_1\omega_2}{k_1} = -\frac{\omega_1}{k_1}\frac{\omega_2^2 - k_1}{\varsigma} = -\frac{\omega_1}{k_1}\frac{\frac{k_1k_2}{\omega_1^2} - k_1}{\varsigma} = \frac{1}{\upsilon_1},$$

$$B_2 = -\frac{\upsilon_1(\upsilon_1\omega_1 - \upsilon_2\omega_2)}{\upsilon_1\omega_2 - \upsilon_2\omega_1} = -\frac{\upsilon_1\omega_1\omega_2}{k_1} = -\frac{\omega_1}{k_1}\frac{\omega_1^2 - k_1}{\varsigma} = -\frac{\omega_1}{k_1}\frac{\frac{k_1k_2}{\omega_2^2} - k_1}{\varsigma} = \frac{1}{\upsilon_2}.$$

When deriving (A.15), Eq. (A.4) and the identities $\omega_1^2\omega_2^2 = k_1k_2$ and $\omega_1^2 + \omega_2^2 = k_1 + k_2 + \varsigma^2$ are used.

Substituting Eqs. (A.15) and (A.12) into (A.14) yields the following expressions for the amplitudes and phase angles:

$$\text{(A.16)}\qquad \dot{a}_i = \varepsilon^{1/2}F_{a,i}^{(0)} + \varepsilon F_{a,i}^{(1)}, \quad \dot{\phi}_i = \varepsilon^{1/2}F_{\phi,i}^{(0)} + \varepsilon F_{\phi,i}^{(1)}, \qquad i = 1, 2,$$

where

$$\text{(A.17)}\quad F_{a,i}^{(0)} = \frac{(-1)^i\varsigma\xi(t)}{\upsilon_i\varpi_{ii}(\omega_2^2 - \omega_1^2)}\Big\{ -\cos\Phi_i\sum_{j=1}^{2}\varpi_{jj}a_j\sin\Phi_j + \zeta\upsilon_i\sin\Phi_i\sum_{j=1}^{2}\varpi_{jj}\upsilon_j a_j\cos\Phi_j\Big\},$$

$$\begin{aligned} F_{a,i}^{(1)} = \frac{(-1)^i\varsigma}{\upsilon_i\varpi_{ii}(\omega_2^2 - \omega_1^2)}\Big\{ &-\cos\Phi_i\Big[2\beta_a\sum_{j=1}^{2}\varpi_{jj}a_j\omega_j\cos\Phi_j - \beta_b\varsigma\sum_{j=1}^{2}\varpi_{jj}\upsilon_j a_j\cos\Phi_j \\ &- \sum_{j=1}^{2}\varpi_{jj}a_j\mathcal{H}[\sin\Phi_j]\Big] - \upsilon_i\sin\Phi_i\Big[2\beta_a\sum_{j=1}^{2}\varpi_{jj}\upsilon_j a_j\omega_j\sin\Phi_j \\ &- \beta_b\varsigma\sum_{j=1}^{2}\varpi_{jj}a_j\sin\Phi_j + \delta\sum_{j=1}^{2}\upsilon_j\varpi_{jj}a_j\mathcal{H}[\cos\Phi_j]\Big]\Big\}, \end{aligned}$$

$$F_{\phi,i}^{(0)} = \frac{(-1)^i\varsigma\xi(t)}{a_i\upsilon_i\varpi_{ii}(\omega_2^2 - \omega_1^2)}\Big\{ \sin\Phi_i\sum_{j=1}^{2}\varpi_{jj}a_j\sin\Phi_j + \zeta\upsilon_i\cos\Phi_i\sum_{j=1}^{2}\varpi_{jj}\upsilon_j a_j\cos\Phi_j\Big\},$$

$$\begin{aligned} F_{\phi,i}^{(1)} = \frac{(-1)^i\varsigma}{a_i\upsilon_i\varpi_{ii}(\omega_2^2 - \omega_1^2)}\Big\{ &-\sin\Phi_i\Big[-2\beta_a\sum_{j=1}^{2}\varpi_{jj}a_j\omega_j\cos\Phi_j + \beta_b\varsigma\sum_{j=1}^{2}\varpi_{jj}\upsilon_j a_j\cos\Phi_j \\ &+ \sum_{j=1}^{2}\varpi_{jj}a_j\mathcal{H}[\sin\Phi_j]\Big] + \upsilon_i\cos\Phi_i\Big[-2\beta_a\sum_{j=1}^{2}\varpi_{jj}\upsilon_j a_j\omega_j\sin\Phi_j \\ &+ \beta_b\sum_{j=1}^{2}\varpi_{jj}a_j\sin\Phi_j - \delta\sum_{j=1}^{2}\upsilon_j\varpi_{jj}a_j\mathcal{H}[\cos\Phi_j]\Big]\Big\}. \end{aligned}$$

Appendix B. Stochastic averaging

This Appendix describes the process of stochastic averaging from the Stratonovich differential equations with polar coordinates in terms of the amplitudes and phase angles in Eq. (A.16) or Eq. (2.5) to Itô differential equations with polar coordinates Eqs. (2.6a) and (2.6b).

The averaging operator is defined as

$$\underset{t}{\mathcal{M}}(\cdot) = \lim_{T\to\infty}\frac{1}{T}\int_t^{t+T}(\cdot)\mathrm{d}t.$$

When applying the averaging operator, the integration is performed over explicitly appearing t only.

Applying the stochastic averaging method to Eq. (A.16) yields

$$\begin{aligned}\mathrm{d}a_i &= \varepsilon\, m_i^a\mathrm{d}t + \varepsilon^{\frac{1}{2}}\sum_{j=1}^{2}\sigma_{ij}^a\mathrm{d}W_j^a,\\ \mathrm{d}\phi_i &= \varepsilon m_i^\phi\mathrm{d}t + \varepsilon^{\frac{1}{2}}\sum_{j=1}^{2}\sigma_{ij}^\phi\mathrm{d}W_j^\phi,\quad i=1,2,\end{aligned}\tag{B.1}$$

where the elements of the drift vector and diffusion matrices are given by

$$\begin{aligned}m_1^a &= \underset{t}{\mathcal{M}}\Big\{F_{a,1}^{(1)} + \int_{-\infty}^{0}\mathsf{E}\Big[\sum_{j=1}^{2}\Big(\frac{\partial F_{a,1}^{(0)}}{\partial a_j}F_{a,j\tau}^{(0)} + \frac{\partial F_{a,1}^{(0)}}{\partial \phi_j}F_{\phi,j\tau}^{(0)}\Big)\Big]\mathrm{d}\tau\Big\}\\ &= a_1E_1 + V_0\Big[(3V_1+2V_3)a_1 + \frac{\varpi_{21}^2D_2a_2^2}{a_1}\Big],\\ m_2^a &= \underset{t}{\mathcal{M}}\Big\{F_{a,2}^{(1)} + \int_{-\infty}^{0}\mathsf{E}\Big[\sum_{j=1}^{2}\Big(\frac{\partial F_{a,2}^{(0)}}{\partial a_j}F_{a,j\tau}^{(0)} + \frac{\partial F_{\phi,2}^{(0)}}{\partial \phi_j}F_{\phi,j\tau}^{(0)}\Big)\Big]\mathrm{d}\tau\Big\}\\ &= a_2E_2 + V_0\Big[(3V_2+2V_3)a_2 + \frac{\varpi_{12}^2D_1a_1^2}{a_2}\Big],\\ b_{11}^a &= \underset{t}{\mathcal{M}}\Big\{\int_{-\infty}^{\infty}\mathsf{E}[F_{a,1}^{(0)}F_{a,1\tau}^{(0)}]\mathrm{d}\tau\Big\} = 2V_0(V_1a_1^2 + \varpi_{21}^2D_2a_2^2),\\ b_{12}^a &= \underset{t}{\mathcal{M}}\Big\{\int_{-\infty}^{\infty}\mathsf{E}[F_{a,1}^{(0)}F_{a,2\tau}^{(0)}]\mathrm{d}\tau\Big\} = 2V_0V_3a_1a_2,\\ b_{22}^a &= \underset{t}{\mathcal{M}}\Big\{\int_{-\infty}^{\infty}\mathsf{E}[F_{a,2}^{(0)}F_{a,2\tau}^{(0)}]\mathrm{d}\tau\Big\} = 2V_0(V_2a_2^2 + \varpi_{12}^2D_1a_1^2),\end{aligned}\tag{B.2}$$

with the constants defined by

$$\begin{aligned}&\varpi_{12} = \frac{\varpi_{11}}{\varpi_{22}},\quad \varpi_{21} = \frac{\varpi_{22}}{\varpi_{11}},\quad V_0 = \frac{\varsigma^2}{16\big(\omega_1^2-\omega_2^2\big)^2},\quad V_1 = \Big(\zeta\upsilon_1 - \frac{1}{\upsilon_1}\Big)^2S(2\omega_1),\\ &V_2 = \Big(\zeta\upsilon_2 - \frac{1}{\upsilon_2}\Big)^2S(2\omega_2),\quad V_3 = 2\zeta S^+ - \Big(\zeta^2\upsilon_1\upsilon_2 + \frac{1}{\upsilon_1\upsilon_2}\Big)S^-,\end{aligned}\tag{B.3}$$

$$D_1=\Big(\zeta^2\upsilon_1^2+\frac{1}{\upsilon_2^2}\Big)S^+-2\frac{\zeta\upsilon_1}{\upsilon_2}S^-,\quad D_2=\Big(\zeta^2\upsilon_2^2+\frac{1}{\upsilon_1^2}\Big)S^+-2\frac{\zeta\upsilon_2}{\upsilon_1}S^-,$$
$$E_1=-\Big(\beta_a+\frac{\varsigma^2(\beta_a-\beta_b)}{\omega_1^2-\omega_2^2}\Big)+\frac{\varsigma}{\varpi_{11}(\omega_1^2-\omega_2^2)}\Big[\frac{\mathcal{M}_t\{\cos\Phi_1\mathcal{H}[q_1]\}}{\upsilon_1}-\delta\mathcal{M}_t\{\sin\Phi_1\mathcal{H}[q_2]\}\Big],$$
$$E_2=-\Big(\beta_a+\frac{\varsigma^2(\beta_a-\beta_b)}{\omega_1^2-\omega_2^2}\Big)-\frac{\varsigma}{\varpi_{22}(\omega_1^2-\omega_2^2)}\Big[\frac{\mathcal{M}_t\{\cos\Phi_2\mathcal{H}[q_1]\}}{\upsilon_2}-\delta\mathcal{M}_t\{\sin\Phi_2\mathcal{H}[q_2]\}\Big].$$

The functions $S^{\pm}$ are defined as follows

$$S^{\pm}=S(\omega_1+\omega_2)\pm S(\omega_1-\omega_2), \tag{B.4}$$

and the function $S(\omega)$ is the cosine power spectral densities of the stochastic process $\xi(t)$.

Assuming the kernel functions $H(t)$ and $t\cdot H(t)$ are integrable over $[0,\infty)$, then applying the transformation $s=t-\tau$ and changing the order of integration lead to [26, 29]

$$\begin{aligned}\mathcal{M}_t[I_i^{\rm cs}]&=\mathcal{M}_t\{\cos\Phi_i\mathcal{H}[\sin\Phi_i]\}=\mathcal{M}_t\Big\{\cos\Phi_i\int_0^t H(t-s)\sin\Phi_i(s)\mathrm{d}s\Big\}\\
&=\lim_{T\to\infty}\frac{1}{T}\int_{t=0}^{T}\int_{s=0}^{t}H(t-s)\cos\Phi_i(t)\sin\Phi_i(s)\mathrm{d}s\,\mathrm{d}t\\
&=\lim_{T\to\infty}\frac{1}{T}\int_{t=0}^{T}\int_{\tau=0}^{t}H(\tau)\cos\Phi_i(t)\sin\Phi_i(t-\tau)\mathrm{d}\tau\,\mathrm{d}t\\
&=\lim_{T\to\infty}\frac{1}{2T}\int_{\tau=0}^{T}\int_{t=\tau}^{T}H(\tau)\big[\sin(2\omega_it-\omega_i\tau+2\bar{\varphi})-\sin\omega_i\tau\big]\mathrm{d}t\mathrm{d}\tau\\
&=-\frac{1}{2}\int_0^{\infty}H(\tau)\sin\omega_i\tau\,\mathrm{d}\tau=-\frac{1}{2}H^s(\omega_i),\quad i=1,2.\end{aligned}$$

Similarly, it is found that

$$\begin{aligned}\mathcal{M}_t\{\cos\Phi_i\mathcal{H}[\sin\Phi_j]\}&=\mathcal{M}_t\Big\{\cos\Phi_i(t)\int_0^t H(t-\tau)\sin\Phi_j(\tau)\mathrm{d}\tau\Big\}\\
&=-\frac{1}{2}\mathcal{M}_t\Big\{\int_0^{\infty}H(\tau)\sin[(\omega_i-\omega_j)\tau+(\phi_i-\phi_j)]\mathrm{d}\tau\Big\}=0,\quad i\neq j,\end{aligned}$$

$$\begin{aligned}\mathcal{M}_t\big[I_i^{\rm cc}\big]&=\mathcal{M}_t\{\cos\Phi_i\mathcal{H}[\cos\Phi_i]\}=\frac{1}{2}H^c(\omega_i),\quad \mathcal{M}_t\{\cos\Phi_i\mathcal{H}[\cos\Phi_j]\}=0,\\
\mathcal{M}_t\big[I_i^{\rm sc}\big]&=\mathcal{M}_t\{\sin\Phi_i\mathcal{H}[\cos\Phi_i]\}=\frac{1}{2}H^s(\omega_1),\quad \mathcal{M}_t\{\sin\Phi_i\mathcal{H}[\cos\Phi_j]\}=0,\\
\mathcal{M}_t\big[I_i^{\rm ss}\big]&=\mathcal{M}_t\{\sin\Phi_i\mathcal{H}[\sin\Phi_i]\}=\frac{1}{2}H^c(\omega_1),\quad \mathcal{M}_t\{\sin\Phi_i\mathcal{H}[\sin\Phi_j]\}=0,\end{aligned} \tag{B.5}$$

where

$$H^s(\omega)=\int_0^{\infty}H(\tau)\sin\omega\tau\,\mathrm{d}\tau,\quad H^c(\omega)=\int_0^{\infty}H(\tau)\cos\omega\tau\,\mathrm{d}\tau \tag{B.6}$$

are the sine and cosine transformations of the viscoelastic kernel function $H(t)$. Combining Eqs. (A.7) and (B.5) results in

$$\begin{aligned}(\text{B.7})\quad &\underset{t}{\mathcal{M}}\{\cos\Phi_i\mathcal{H}[q_1]\} = -\frac{1}{2}\varpi_{ii}a_iH^s(\omega_i), \quad \underset{t}{\mathcal{M}}\{\sin\Phi_i\mathcal{H}[q_1]\} = \frac{1}{2}\varpi_{ii}a_iH^c(\omega_i),\\ &\underset{t}{\mathcal{M}}\{\sin\Phi_i\mathcal{H}[q_2]\} = \frac{1}{2}\varpi_{ii}\upsilon_ia_iH^s(\omega_i), \quad \underset{t}{\mathcal{M}}\{\cos\Phi_i\mathcal{H}[q_2]\} = \frac{1}{2}\varpi_{ii}\upsilon_ia_iH^c(\omega_i).\end{aligned}$$

Substituting Eq. (B.7) into (B.3) produces

$$\begin{aligned}E_1 &= -\Big(\beta_a + \frac{\varsigma^2(\beta_a-\beta_b)}{\omega_1^2-\omega_2^2}\Big) - \frac{1}{2}\frac{\varsigma H^s(\omega_1)}{\omega_1^2-\omega_2^2}\Big(\frac{1}{\upsilon_1}+\delta\upsilon_1\Big),\\ E_2 &= -\Big(\beta_a + \frac{\varsigma^2(\beta_a-\beta_b)}{\omega_1^2-\omega_2^2}\Big) + \frac{1}{2}\frac{\varsigma H^s(\omega_2)}{\omega_1^2-\omega_2^2}\Big(\frac{1}{\upsilon_2}+\delta\upsilon_2\Big),\end{aligned}$$

which may be called pseudo-damping coefficients. In this study, the viscoelastic kernel function is supposed to follow ordinary Maxwell model

$$(\text{B.8})\qquad H(t) = \gamma e^{-\eta t},$$

where γ and η are the coefficient of the viscoelasticity and the relaxation, respectively. γ represents the intensity of material relaxation, η characterizes the material relaxation rate. The sine and cosine transformations in Eq. (B.6) are given by

$$H^s(\omega) = \frac{\omega\gamma}{\eta^2+\omega^2}, \quad H^c(\omega) = \frac{\gamma\eta}{\eta^2+\omega^2}.$$

References

1. W. Nagata, N. Sri Namachchivaya, *Bifurcations in gyroscopic systems with an application to rotating shafts*, Proc. R. Soc. Lond., Ser. A, Math. Phys. Eng. Sci. **454** (1998), 543–585.
2. C. D. Mote Jr, *A study of band saw vibrations*, J. Franklin Inst. **279**(6) (1965), 430–444.
3. C. D. Mote Jr, S. Naguleswaran, *Theoretical and experimental band saw vibrations*, J. Manuf. Sci. Eng. **88**(2) (1966), 151–156.
4. S. Naguleswaran, C. J. Williams, *Lateral vibrations of band saw blades, pulley belts and the like*, Int. J. Mech. Sci. **10** (1968), 239–250.
5. A. G. Ulsoy, C. D. Mote Jr, *Vibration of wideband saw blades*, J. Manuf. Sci. Eng. **104**(1) (1982), 71–78.
6. S. F. Asokanthan, *Parametric Instabilities in Saw Blades*, PhD thesis, University of Waterloo, Waterloo, Canada, 1986.
7. M. G. Yin, *Lyapunov Exponents and Stochastic Stability of Linear Gyroscopic Systems*, Master thesis, University of Waterloo, Waterloo, Canada, 1991.
8. R. Z. Khasminskii, *Stochastic Stability of Differential Equations*, Kluwer Academic Publishers, Norwell, 1980.
9. N. M. Abdelrahman, *Stochastic Stability of Viscoelastic Dynamical Systems*, University of Waterloo, Waterloo, Canada, 2002.
10. R. Pavlovic, I. R. Pavlovic, *Dynamic stability of Timoshenko beams on Pasternak viscoelastic foundation*, Theor. Appl. Mech. **45**(1) (2018), 67–81.
11. Y. Zhou, K. Huang, *Static and dynamic stabilities of modified gradient elastic Kirchhoff–Love plates*, Eur. J. Mech., A, Solids **108** (2024), 105426.
12. J. Deng, *Numerical simulation of stability and responses of dynamic systems under parametric excitation*, Appl. Math. Modelling **119** (2023), 648–676.
13. Y. K. Lin, G. Q. Cai, *Probabilistic Structural Dynamics*, McGraw-Hill, 2004.
14. W. C. Xie, *Dynamic Stability of Structures*, Cambridge University Press, Cambridge, 2006.

15. V. Stojanovic, J. Deng, M. D. Petkovic, M. A.Ristic, *Modeling of Complex Dynamic Systems: Fundamentals and Applications*, Elsevier, 2025.
16. P. Kozic, *Stability of the moments of double parametric random excitation of a damped Mathieu oscillator*, Theor. Appl. Mech. **14** (1988), 45–50.
17. P. Baxendale, D. Stroock, *Large deviations and stochastic flows of diffeomorphisms*, Probab. Theory Relat. Fields **80** (1988), 169–215.
18. L. Arnold, M. M. Doyle, N. Sri Namachchivaya, *Small noise expansion of moment Lyapunov exponents for two-dimensional systems*, Dyn. Stab. Syst. **12**(3) (1997), 187–122.
19. R. Z. Khasminskii, N. Moshchuk, *Moment Lyapunov exponent and stability index for linear conservative system with small random perturbation*, SIAM J. Appl. Math. **58**(1) (1998), 245–256.
20. N. Sri Namachchivaya, H. J. Van Roessel, *Moment Lyapunov exponent and stochastic stability of two coupled oscillators driven by real noise*, J Appl. Mech. **68**(6) (2001), 903–914.
21. N. L. Vedula, *Dynamics and Stability of Parametrically Excited Gyroscopic Systems*, PhD. thesis, University of Illinois at Urbana-Champaign, Champaign, USA, 2005.
22. J. Deng, Z. Zhong, A. Liu, *Stochastic stability of viscoelastic plates under bounded noise excitation*, Eur. J. Mech., A, Solids **78** (2019), 103849.
23. V. Stojanovic, J. Deng, D. Milic, M. D. Petkovic, *MDOF stochastic stability analysis and applications to a coupled rotating shaft system*, Probab. Eng. Mech. **74** (2023), 103509.
24. R. Pavlovic, P. Kozic, S. Mitic, *Stochastic stability of a linear viscoelastic beam under time and space-dependent loading*, Theor. Appl. Mech. **25** (1999), 91–106.
25. S. T. Ariaratnam, *Stochastic stability of linear viscoelastic systems*, Probab. Eng. Mech. **8**(3–4) (1993), 153–155.
26. S. T. Ariaratnam, *Stochastic stability of viscoelastic systems under bounded noise excitation*, In: A. Naess, S. Krenk (eds.), *IUTAM Symposium on Advances in Nonlinear Stochastic Mechanics*, 11–18, Kluwer Academic Publishers, 1996.
27. W. C. Xie, *Moment Lyapunov exponents of a two-dimensional viscoelastic system under bounded noise excitation*, J Appl. Mech. **69**(3) (2002), 346–357.
28. Q. Huang, W. C. Xie, *Stability of SDOF linear viscoelastic system under the excitation of wide-band noise*, J. Appl. Mech. **75**(2) (2008), 021012.
29. G. S. Larionov, *Investigation of the vibration of relaxing systems by the averaging method*, Polym. Mech. **5** (1969), 714–720.
30. G. Q. Cai, W. Q. Zhu, *Elements of Stochastic Dynamics*, World Scientific Publishing, 2017.
31. W. Q. Zhu, M. L. Deng, G. Q. Cai, *Stochastic Averaging Methods and Applications*, Volume 1, Springer Singapore, 2025.
32. J. Deng, W. C. Xie, M. D. Pandey, *Moment Lyapunov exponent and stochastic stability of coupled viscoelastic systems under white noise excitation*, J. Mech. Mater. Struct. **9**(1) (2014), 27–50.
33. A. Wolf, J. B. Swift, H. L. Swinney, J. A. Vastano, *Determining Lyapunov exponents from a time series*, Physica D **16**(3) (1985), 285–317.
34. S. T. Ariaratnam, S. F. Asokanthan, *Instabilities in moving bands under random tension fluctuation*, J. Sound Vib. **167**(3) (1993), 421–432.
35. W. C. Xie, *Differential Equations for Engineers*, Cambridge University Press, Cambridge, 2010.
36. E. Wedig, *Lyapunov exponent of stochastic systems and related bifurcation problems*, In: S. T. Ariaratnam, G. I. Schuëller (eds.), *Stochastic Structural Dynamics: Progress in Theory and Applications*, 315–317, Elsevier Applied Science, London, 1988.

СТОХАСТИЧКА СТАБИЛНОСТ ГИРОСКОПСКИХ ВИСКЕОЛАСТИЧНИХ СИСТЕМА И ПРИМЕНЕ У АКСИЈАЛНО ПОКРЕТНИМ ТРАКАМА

Резиме. Овај рад истражује стохастичку стабилност гироскопских вискоеластичних система подвргнутих параметарској побуди широкопојасним шумом. Анализа се фокусира и на стабилност момената, користећи Љапуновљеве експоненте, и на скоро сигурну стабилност, путем највећег Љапуновљевог експонента. Разматрани широкопојасни шумови укључују Гаусов бели шум и Орнштајн-Уленбеков шум. Прво се Стратоновићеве стохастичке диференцијалне једначине, које описују систем са малим пригушењем и слабим побуђивањем, претварају у Итоове стохастичке диференцијалне једначине помоћу техника стохастичког усредњавања. Затим се уводи елегантан математички оквир за апроксимацију Љапуновљевих експонената момената путем стохастичких трансформација и проблема сопствених вредности. Највећи Љапуновљев експонент се потом изводи на основу његовог односа са Љапуновљевим експонентима момената. Пример примене укључује извођење стохастичких једначина кретања за аксијално покретни систем трака са флуктуирајућим напоном, анализирајући његову стохастичку стабилност. Аналитичке апроксимације су проверене путем Монте Карло симулација и упоређене са резултатима из литературе. Студија такође разматра утицај различитих параметара на стабилност система, са потенцијалним применама у инжењерским областима.

Department of Civil Engineering
Lakehead University
Thunder Bay
Ontario
Canada
jdeng2@lakeheadu.ca
https://orcid.org/0000-0002-1487-1646

University of Waterloo
Waterloo
Ontario
Canada
xie@uwaterloo.ca
https://orcid.org/0000-0002-9761-7968

(Received 27.11.2025)
(Revised 05.02.2026)
(Available online 08.05.2026)